Running Title: A human stem cell model of mixoid liposarcoma.

Expression of FUS-CHOP fusion protein in immortalized/transformed human Mesenchymal Stem Cells drives mixoid liposarcoma formation

Rene Rodriguez[1*], Juan Tornin[1], Carlos Suarez[1], Aurora Astudillo[2], Ruth Rubio[3], Carole Yauk[4], Andrew Williams[4], Michael Rosu-Myles[5], Juan M. Funes[6], Chris Boshoff[6] & Pablo Menendez[3,7,8*]

[1]Hospital Universitario Central de Asturias and Instituto Universitario de Oncología del Principado de Asturias, Oviedo, 33006, Spain. [2]Servicio de Anatomía Patológica, Hospital Universitario Central de Asturias, Oviedo, 33006, Spain. [3]GENYO, Centre for Genomics and Oncological Research: Pfizer / University of Granada / Andalusian Regional Government, Granada, 18016, Spain; [4]Environmental Health Science and Research Bureau, Healthy Environments and Consumer Safety Branch, Health Canada, Ottawa, ON, Canada. [5]Health Canada Centre for Biologics Research, Biologics and Genetic Therapies Directorate, Health Canada, Ottawa, ON, Canada. [6]UCL Cancer Institute, Paul O'Gorman Building, University College London, London, UK. [7]Josep Carreras Leukemia Research Institute-Cell Therapy Program, Facultat de Medicina. University of Barcelona, Barcelona, 08036, Spain; [8] Institució Catalana de Reserca i Estudis Avançats (ICREA).

Author contributions: **R.Ro**: conceived the study, designed the study, performed experiments, analyzed the data, interpreted the results and wrote the paper. **J. T, R.Ru**: performed experiments. **C.S, A.A, C.Y, A.W & M.R-M**: analyzed data and interpreted the results. **J.M.F & C.B**: provided key biological material. **P.M**: conceived the study, analyzed the data, interpreted the results and wrote the paper. **P.M, M.R-M and R.Ro** financially supported the study.

[*]**Correspondence should be addressed to:**
Pablo Menendez Ph.D.
Josep Carreras Leukemia Research Institute. Facultat de Medicina. University of Barcelona. Carrer de Casanova 143. 08036. Barcelona. Spain.
GENyO. Centre for Genomics and Oncological Research: Pfizer / University of Granada / Andalusian Regional Government. 18007. Granada. Spain.
Email: pmenendez@carrerasresearch.org; pablo.menendez@genyo.es

Rene Rodriguez Ph.D.
Hospital Universitario Central de Asturias and Instituto Universitario de Oncología del Principado de Asturias. Laboratorio 2 ORL–IUOPA. C/ Celestino Villamil s/n, 33006 Oviedo, SPAIN.
Phone: 00 34 985 10 80 00 (ext 38524) / Fax: 00 34 985 10 80 15
Email: renerg@ficyt.es

Pablo Menendez and Rene Rodriguez share senior authorship

Acknowledgments: we thank the Andalusian Platform of Bioinformatics (PAB; University of Málaga) for providing access to IPA software and Dr. Patrick Aebischer for the pLVUHshp53 plasmid. This work was supported by the Instituto de Salud Carlos III/Fondos FEDER (PI10/00449 to P.M, CP11/00024 to R.Ro, Tercel (RD12/0019/0006) and RTICC (RD12/0036/0015)), the Junta de Andalucía/FEDER (P08-CTS-3678 to P.M), the Spanish Association Against Cancer (Junta Provincial de Albacete-CI110023 to P.M and Junta Provincial de Granada to R.Ro), Grupo Español de Investigación en Sarcomas (beca J.M. Buesa-2012 to R. Ro), Health Canada (H4084-112281

to P.M, R.Ro, and M.R-M), Health Canada's Genomics Research and Development Initiative (to M.R-M, C.Y and A.W) and Obra Social Cajastur-IUOPA. R.Ro is supported by the Miguel Servet program of the ISCIII/FEDER. R.Ru was supported by a fellowship of the ISCIII/FEDER. P.M is an ICREA Research Professor supported by the Generalitat of Catalunya.

Key words: MSCs, mixoid liposarcoma, FUS-CHOP, oncogenic hits, sarcomagenesis.

ABSTRACT

Increasing evidence supports that mesenchymal stromal/stem cells (MSCs) may represent the target cell for sarcoma development. Although different sarcomas have been modeled in mice upon expression of fusion oncogenes in MSCs, sarcomagenesis has not been successfully modeled in human MSCs (hMSCs). We report that FUS-CHOP, a hallmark fusion gene in mixoid liposarcoma (MLS), has an instructive role in lineage commitment, and its expression in hMSC sequentially immortalized/transformed with up to 5 oncogenic hits (p53 and Rb deficiency, hTERT over-expression, c-myc stabilization and H-RAS^{v12} mutation) drives the formation of serially transplantable MLS. This is the first model of sarcoma based on the expression of a sarcoma-associated fusion protein in hMSC, and allowed us to unravel the differentiation processes and signaling pathways altered in the MLS-initiating cells. This study will contribute to test novel therapeutic approaches, and constitutes a proof-of-concept to employ hMSCs as target cell for modeling other fusion gene-associated human sarcomas.

INTRODUCTION

It has been recently established that transformed mesenchymal stem cells (MSCs) may act as tumor initiating cells (TIC) capable of initiating sarcomagenesis *in vivo*. Accordingly, many efforts have been undertaken to characterize the transformation process of MSCs, and to prospectively generate models for different sarcomas based on MSCs, which would constitute an unprecedented system to understand the mechanisms underlying sarcomagenesis and to search target-specific therapies [1-3]. Among the different types of sarcomas, those characterized by the presence of tumor-specific fusion oncogenes as a result of chromosomal translocations constitute an active field of research. Several types of tumors resembling human sarcomas have been reproduced *in vivo* using transgenic mouse models, and also upon the expression of sarcoma-specific fusion proteins in mouse MSC (mMSCs). Specifically, Ewing Sarcoma [4, 5], myxoid liposarcoma, [6-9] alveolar rhabdomyosarcoma [10, 11] and synovial sarcoma [12] have been reproduced upon expression in mouse cells of EWS-FLI-1, FUS-CHOP (FC), PAX-FKHR and SYT-SSX, respectively. However, previous efforts to model sarcomagenesis using human MSC (hMSCs) failed to reproduce the tumor phenotype. For example, the expression of the fusion proteins EWS-FLI-1 or SYT-SSX1 in hMSCs induced a transcriptional expression pattern similar to that observed in Ewing´s Sarcomas [13] or synovial sarcoma [14], respectively, but did not cause cell transformation. In fact, no fusion gene-based model of sarcoma has been developed so far using hMSCs as target cells. The “multiple hit” model of cancer suggests that, at least in mesenchymal cancer (leukemias and sarcomas), a fusion oncogene may act as an initiating oncogenic event by blocking a particular differentiation pathway whereas secondary cooperating hits that most likely affect proliferation/apoptosis, may be required to render a fully transformed phenotype [15].

Myxoid liposarcomas (MLS) represent about one third of liposarcomas and account for approximately 10% of all adult soft tissue sarcomas. MLS occurs predominantly in patients aged

30 to 50 years old, and shows a high tendency to recur locally or to metastasize to other soft tissue locations [16]. A proportion of cases show histological progression to a subclass of MLS displaying round-cell morphology, a feature significantly associated with a poor prognosis. Five year survival rates varies between 20-60%, depending in part on the round-cell histology progression [16]. MLS is characterized by the recurrent translocation t(12;16)(q13;p11), which fuses FUS (FUsed in Sarcoma; also termed TLS, Translocated in LipoSarcoma) to CHOP (C/EBP HOmologous Protein; also termed DDIT3, DNA Damage-Inducible Transcript 3) on chromosome 12. The NH2-terminal domain of FUS confers the transactivation domain to the fusion protein [17]. CHOP is a member of the C/EBP (CCAAT/Enhancer Binding Proteinα) family of transcription factors and heterodimerizes with, and inactivates other C/EBP members [18]. FUS-CHOP (FC) fusion protein is believed to repress the development of adipocytic precursors by repressing PPARγ (Peroxisome Proliferator-Activated Receptor γ) and C/EBP, causing disruption of differentiation and the development of MLS [19].

We previously showed that the expression of FC in transformed leiomyosarcoma-forming p53-deficient adipose tissue-derived mMSCs (ASCs) [20] redirects the tumor genesis/phenotype towards the formation of liposarcoma-like tumors [9]. However, in the human setting, the expression of FC fails to transform either wt or p53-deficient hASCs [9]. Here, we take advantage of an available collection of sequentially mutated human bone marrow MSCs (BM-hMSCs) ranging from wt (no oncogenic hits) to fully transformed hMSCs (targeted with 5 oncogenic mutations) [21] to address whether expression of FC in BM-hMSCs harboring different oncogenic lesions cooperates to develop a *bona fide* hMSC-based model reproducing the MLS phenotype. Importantly, most of these oncogenic hits or their downstream signaling pathways are among the few genetic alterations, apart from the FC translocation, described in human MLS to date (see Discussion). Overall, we have developed and characterized a model of MLS based on the expression of FC in

transformed hMSCs. This study provides the first human model of sarcomagenesis based on the expression of a fusion oncogene in hMSCs.

MATERIALS AND METHODS

Generation and culture of mutated human BM-hMSCs

Wild type or "0-hits" BM-hMSCs (wt-MSCs or MSC-0H) were obtained from Inbiobank (www.inbiobank.org; San Sebastian, Spain) upon signed informed consent. Wt-MSCs depleted of p53 (MSC-1H) **(Fig. S1)** were generated by transduction with lentiviral particles carrying a p53-shRNA expression vector (pLVUH-shp53; Addgene plasmid 11653; [22]) as previously described [9]. The BM-hMSCs carrying 3, 4 or 5 different oncogenic hits (MSC-3H, MSC-4H and MSC-5H) were developed and characterized elsewhere [21]. **Fig 1A** summarizes the genotype/oncogenic hits of each hMSC type used in this study. To over-express FC, each type of BM-MSCs (MSC-0H to -5H) was infected overnight with concentrated viral particles expressing either pRRL-EF1α-PGK-GFP (empty vector; GFP) or pRRL-EF1α-FUS-CHOP-PGK-GFP (FC expressing vector; FC) as previously reported **(Fig. S2A)** [9]. The transduction efficiency (50-96%) was analyzed by flow cytometry (% GFP+ cells) **(Fig. S2B)**. All the resulting MSC-GFP and MSC-FC cell lines were cultured and immunophenotypically characterized as previously described [9, 23].

MSC differentiation

MSCs were plated in 6-well plates and allowed to grow to confluence. Culture medium was then replaced with specific differentiation inductive media. For adipogenic differentiation cells were cultured in adipogenic MSC Differentiation BulletKit (Lonza, Basel, Switzerland) for 7 or 14 days. Differentiated cell cultures were stained with Oil Red O (Sigma, St. Louis, MO) [24] and the level of differentiation was quantified by extracting the stain with isopropanol and measuring the absorbance at 510 nm. For osteogenic differentiation, cells were cultured in Osteogenic MSC Differentiation BulletKit (Lonza) for 14 days, and the presence of calcium deposits in differentiated cells was checked by Alizarin red S staining [24].

RT-PCR

Total RNA was extracted from undifferentiated or adipogenic differentiated MSC cultures as well as from human MLS tissue samples obtained upon signed informed consent and first-strand cDNA synthesis was performed using the First-Strand cDNA Synthesis Kit (GE Healthcare, Pittsburgh, PA). The expression of FC and GAPDH was checked by end-point PCR as previously described [9]. The expression of FC, PPARγ (total and isoform 2), C/EBPα, C/EBPδ, LPL, MDM2, CDK2 and MET was assessed by Q-PCR using SYBR Green PCR Kit (Qiagen, Valencia, CA) [25]. GAPDH was used as a housekeeping gene. The following PCR conditions were used: 5 min at 94ºC, 35 cycles of 30 seconds at 94ºC followed by 50 seconds at 60ºC and 50 seconds at 72ºC and a final extension of 10 min at 72ºC. Primer sequences used are shown in **Table S1.**

Western Blot

Whole cell protein extraction and western blot analysis were done as previously described [26]. Antibodies used were as follows: anti-p53 [(sc-126), 1:500 dilution], anti-GADD153/CHOP [(sc-7351), 1:200; used for the detection of FC], anti-PPARγ-2 [(sc-166731), 1:200 dilution] and anti-C/EBPδ [(sc-636), 1:200 dilution] from Santa Cruz Biotechnology (Santa Cruz, CA); anti-FUS/TLS [(A300-292A), 1:7000] from Bethyl Laboratories (Montgomery, TX); and anti-β-Actin [(A-1978), 1:20.000] (Sigma).

***In vivo* tumorogenesis assays**

NOD/SCID IL2Rγ$^{-/-}$ mice were obtained from Jackson Laboratories (Bar Harbor, ME). All mice were housed under specific pathogen-free conditions, fed *ad libitum* and maintained under veterinary care according to animal welfare facilities guidelines. Animals were used at 8-12 weeks of age. Mice were inoculated subcutaneously with 5x10^6 MSCs or 1x10^6 primary tumor-derived cells. Animals were sacrificed when tumors reached approximately 1 cm^3 or 5 months after infusion. All

animal research protocols were approved by the Animal Research Ethical Committee of the University of Granada prior to the study. Upon tumor removal, half of the tumor was mechanically disaggregated to establish *ex-vivo* tumor cell lines as described [20]. The remaining portion of the tumor was used for immunohistopathology analysis.

Histological analysis

Tumor samples were fixed in formol, embedded in paraffin, cut into 4μm sections and stained with haematoxylin and eosin. Multiple tumor sections were stained with specific antibodies against GFP (1:400 dilution; Molecular Probes, Eugene, OR) or S-100 (1:500; DakoCytomation, Glostrup, Denmark) as previously described [27, 28].

Gene expression profiling (GEP) analysis

MSCs were collected in RNA later (Ambion, Austin, TX) solution until RNA extraction. RNA was isolated using the Agilent Total RNA Isolation Kit (Agilent Technologies, Santa Clara, CA). Sample purity was checked to ensure that A260/280 ratios for all of the RNA samples were ≥ 2. Only RNA samples with RNA integrity ≥ 9 were used in the analysis as determined using an Agilent 2100 Bioanalyzer (Agilent Technologies). RNA was amplified using Agilent Fluorescent Linear Amplification kits (Agilent Technologies), and the cRNA of experimental samples was labeled with Cyanine 5-CTP. Universal reference total RNA (Stratagene, Mississauga, ON, Canada) was labeled with Cyanine 3-CTP. Samples were hybridized to Whole Human Genome 8x60K Microarray (G4851A) and arrays were scanned using an Agilent G2505B scanner (Agilent Technologies). Data were extracted using Feature Extraction software version 10.7.3.1. (Agilent Technologies) and array quality was evaluated using metrics established in Feature Extraction. All pre-processing of the data was conducted using the R software. The median signal intensities for the expression arrays were normalized using the global lowess method using the transform.madata

function in the MAANOVA library. Differentially expressed genes were identified using the MAANOVA library using the Fs statistic. The p-values for all the statistical tests were estimated using the permutation method (30,000 permutations with residual shuffling). These p-values were then adjusted for multiple comparisons by using the false discovery rate approach (FDR). The least-squares means were used to estimate the fold changes for each pairwise comparison. Data from the sample channel only (Cy5) was background subtracted and was normalized using cyclic-lowess normalized followed by collapsing the data to the Gene Symbol using the median. This was done to compare the data from an Affymetrix study (GSE21122) obtained from National Center for Biotechnology Information Gene Expression Omnibus site (http://www.ncbi.nlm.nih.gov/projects/geo). These data were normalized using RMA using the Affy library in Bioconductor, and then collapsed to the gene symbol using the median. The two datasets were merged together using the gene symbol and a linear model was applied to control for differences between two studies. The adjusted data were then collapsed by tumour type and hierarchical clustering using the dissimilarity matrix based on one minus the Pearson correlation with average linkage was performed. This analysis was conducted using the gene symbols that were significantly expressed in the above analysis. Analysis of canonical pathways and upstream regulators significantly altered by FC was performed with the list of differentially expressed genes using Ingenuity Pathway Analysis (IPA) software 8.0 (Ingenuity Systems, Inc., Redwood City, CA). Microarray data have been deposited and are available in Gene Expression Omnibus (http://www.ncbi.nlm.nih.gov/geo/; GSE48030).

RESULTS

The expression of FC in immortalized/transformed hMSCs initiates MLS *in vivo*.

To test whether the expression of FC in immortalized/transformed hMSCs results in liposarcoma formation similar to that observed in the mouse setting [9], we used several sequentially mutated BM-hMSCs ranging from wt (MSC-0H) to fully transformed hMSCs (targeted with up to 5 oncogenic mutations; MSC-5H) **(Table S2)** [21]. These oncogenic hits include: (i) p53 inactivation achieved by p53-shRNA or by expression of the E6 antigen of the HPV-16, (ii) Rb inactivation induced by expression of the E7 antigen of the HPV-16, (iii) ectopic expression of hTERT, (iv) introduction of the SV40 small T antigen to inactivate the PPA2 phosphatase leading to stabilization of c-myc, and (v) expression of oncogenic H-RAS (H-RAS^{v-12}) **(Fig. 1A)**. Most of these oncogenic lesions or their related signaling pathways are among the few relevant alterations previously described in human MLS (see Discussion). The distinct hMSC types were transduced with GFP- (control) and GFP/FC-expressing lentiviral particles, and the expression of FC transcript and protein was verified by RT-PCR **(Fig. 1B)** and Western blot **(Fig. 1C)** using an anti-GADD153/CHOP antibody, which recognizes a 74-kDa band corresponding to FC. There are differences in the level of expression of FC achieved in the different MSCs; however, a range of FC expression is also observed in human MLS samples. The expression of FC in MSC-0H and MSC-1H is in the lower limit of the range of FC expression observed in a panel of human MLS samples (MLS#1 to #6), while the expression of FC in MSC-3H is in the middle of the range, and the expression of FC in MSC-4H and MSC-5H is in the upper limit **(Fig 1 D)**. In any case, the expression of FC did not influence either proliferation or cell death among the distinct MSC types **(Fig. S3)**. Phenotypically, all hMSC types, regardless of the number of oncogenic hits they carry and the FC expression, displayed a typical MSC phenotype: CD90+, CD73+, CD105+, CD166+, CD44+, CD45-, CD34-, CD14-, CD19-, CD106- and HLA-DR- **(Table S3)**.

To assay the *in vivo* tumorogenic potential, NOD/SCID IL2Rγ$^{-/-}$ mice were inoculated subcutaneously with hMSCs of the different genotypes. Independent of FC expression, MSC-0H, MSC-1H and MSC-3H were unable to initiate tumorogenesis *in vivo*. Similarly, MSC-4H-GFP did not developed tumors either **(Table 1)**. However, FC expression in MSC-4H (MSC-4H-FC) initiated tumor formation with 85% penetrance, and a latency of 138±32 days. Histological analysis of the MSC-4H-FC-derived tumors classified these tumors as MLS displaying large areas of small spindle/round cells dispersed within a myxoid matrix and showing the characteristic plexiform vascular pattern and some degree of fatty differentiation including the presence of atypical lipoblasts. Some of these tumors also presented areas of closely-packed high grade small blue cells, characteristic of the round-cell subtype of MLS. (**Fig. 1E & Table 1**). These experimentally induced MLS closely resembled human MLS **(Fig. S4)** and stained positive for S-100, a marker reported to be positive in most cases of MLS [29] **(Fig. S5)**. Interestingly, both MSC-5H-GFP and MSC-5H-FC cells developed aggressive tumors *in vivo* with 100% penetrance, and very short latency (25 days) **(Table 1)**. Histological analysis classified the MSC-5H-GFP-derived tumors as undifferentiated tumors resembling spindle cell sarcomas (UPCS) **(Fig. 1F & Table 1)**. However, the tumors derived from MSC-5H-FC cells showed together with undifferentiated zones, large areas displaying the main features observed in human MLS **(Fig. 1G, Table 1, Fig S4 & Fig. S5)**. In all cases, tumor areas stained positive for GFP, confirming the hMSC origin **(Fig. 1E-G)**.

We next investigated whether genes previously associated to human MLS such as MDM2, CDK2 or MET [8, 30-32] were also upregulated in FC-expressing hMSCs. MDM2 was only slightly upregulated in MSC-4H-FC, MSC-5H-FC as well as in human MLS samples (MLS#5), and CDK2 and MET showed variable levels of overexpression in MSC-1H-FC to MSC-5H-FC and MLS#5 **(Fig S6)**.

Together, these data indicate that FC expression in immortalized, non-transformed MSC-4H (p53 and Rb inactivation, hTERT expression and c-myc stabilization) originates tumors *in vivo*

resembling the histological and molecular features of human MLS, whereas FC expression in transformed MSC-5H (MSC-4H plus H-RAS^{V12}) is capable of redirecting tumor genesis/phenotype from a UPCS to a MLS phenotype, also recapituling the histological/molecular features of human MLS.

Primary FC-expressing MLS are transplantable into secondary NOD/SCID mice.

To determine whether the experimentally induced MLS can be serially transplanted, primary tumors formed from MSC-5H-FC or MSC-4H-FC cells as well as from MSC-5H-GFP cells were mechanically disaggregated and placed back in MSC culture conditions to establish immortalized cell lines (T-5H-GFP#1 to #3, T-5H-FC#1 to #3 and T-4H-FC#1 and #2). These *ex vivo*-established cell lines retained FC expression **(Fig. 2A-B)** at levels comparable to human MLS samples **(Fig 2C)** and displayed identical morphology to the parental MSC-4H and MSC-5H cells. Upon inoculation into secondary recipients, all of the *ex vivo* established cell lines were able to generate tumors *in vivo* with a 100% penetrance and with a short latency period of 15 days for T-5H cells and 38 days for T-4H cells (**Fig. 2D)**. Histopathological analysis of the secondary tumors generated from T-5H-FC and T-4H-FC lines revealed that they retained the main features of human MLS observed in the primary tumors including the presence of large areas of mixoid matrix containing atypical lipoblasts and a plexiform vascular pattern together with varying amounts of the round-cell histological subtype (**Fig. 2E-F**). Additionally, hierarchical clustering of the GEP of T-5H-GFP and T-5H-FC cell lines **(Fig. 2G)** together with a previously published human sarcoma GEP data sets [33] showed that T-5H-FC cells cluster more closely with human MLS tumors. The *in vivo* development of serially transplantable tumors with a phenotype and transcriptome similar to that of primary human MLS demonstrates that the expression of FC in immortalized (MSC-4H) or transformed (MSC-5H) hMSCs provides a *bona fide* model of human MLS.

FC expression and the accumulation of oncogenic lesions block the adipogenic differentiation potential of hMSCs

A blockage of the adipogenic differentiation pathway appears to be a hallmark of liposarcoma development [34]. We investigated how the expression of FC and the sequential accumulation of specific oncogenic mutations affect the adipogenic differentiation potential of hMSCs. After 14 days of culture in adipogenic-inductive conditions, MSC-0H-GFP cultures displayed abundant lipid droplets filled adipocyte-like cells **(Fig. 3A)**. In contrast, MSC-3H and MSC-4H cells displayed an impaired pattern of differentiation in which most cells of the culture presented a small amount (1 to 5) of lipid droplets in their cytoplasm, whereas MSC-5H cultures barely showed even these partially differentiated cells **(Fig. 3A)**. Quantification of the Oil Red staining provided evidence that adipogenic differentiation ability decreased gradually with the introduction of oncogenic lesions **(Fig. 3B)**. Importantly, the expression of FC caused a 30% reduction in the adipogenic differentiation potential of MSC-0H cells **(Fig. 3A,B)**. In addition, T-4H and T-5H tumoral cell lines showed negligible adipogenic differentiation potential in keeping with the parental MSC-4H and MSC-5H **(Fig. 3B-C)**. Notably, MSC-4H and MSC-5H cells, regardless of FC expression, retained full ability to differentiate towards the osteoblastic lineage, suggesting that the introduction of the oncogenic events specifically interfere with adipogenic differentiation **(Fig S7)**.

Previous reports have shown that FC represses master transcription factors controlling adipogenesis such as peroxisome proliferator-activated receptor γ (PPARγ) and CCAAT/enhancer binding protein α (C/EBPα) [19]. Thus, to further investigate the molecular basis of the adipogenic inhibition observed in our hMSC-based MLS model, the expression of master adipogenic factors was analyzed in MSC-0H, MSC-5H and T-5H cells after 0, 7 and 14 days in adipogenic inductive culture conditions. At the transcriptional level, the activation of the master adipogenic transcription factors PPARγ-2 and C/EBPα was heavily repressed by the expression of FC in the MSC-0H cells

(**Fig. 4A**). This strong inhibition was also observed after the accumulation of mutations (i.e. MSC-5H and T-5H cells **(Fig. 4A)**), indicating that oncogenic transformation of hMSCs disrupts the differentiation program. Interestingly, the expression of the early adipogenic transcription factor C/EBPδ was barely affected by the expression of FC and/or further cooperating oncogenic mutations **(Fig. 4A)**. These findings were confirmed at the protein level for both PPARγ-2 and C/EBPδ. PPARγ-2 showed less activation throughout adipogenic differentiation in MSC-0H-FC cells as compared to MSC-0H-GFP cells, and was not activated throughout the adipogenic differentiation of MSC-5H or T-5H cells regardless of the expression of FC **(Fig. 4B)**. However, C/EBPδ displayed similar up-regulation during the adipogenic differentiation process in all of the hMSC types **(Fig. 4B)**. As a result of the FC-mediated inhibition of PPARγ-2 and C/EBPα, the expression of factors specific to terminal adipogenic differentiation, such as lipoprotein lipase (LPL) was also repressed in MSC-0H upon expression of FC **(Fig. 4A)**, confirming the functional blockage of adipogenic differentiation potential observed in MSC-0H-FC (**Fig. 3B**). This repression of LDL was almost complete in MSC-5H and T-5H cells **(Fig. 4A)**. Together, these data indicate that either FC expression or the accumulation of oncogenic hits disrupts the terminal adipogenic differentiation of hMSCs, likely contributing to the development of liposarcoma.

To increase our understanding of the impaired adipogenic differentiation program in our MLS model, we performed whole genome gene expression profiles (GEP) to identify genes altered (differentially expressed) in MSC-0H-FC, MSC-5H-FC and T-5H-FC cell types compared to the control MSC-0H-GFP cells. Using Ingenuity Pathway Analysis (IPA) we searched for adipogenic regulators that were significantly altered among the differentially expressed genes. In the MSC-0H-FC cells, several regulators, including the most important early (C/EBPβ and C/EBPδ) and late (PPARγ and C/EBPα) adipogenic factors, were altered **(Fig. 5A)**. However, many more regulators were up/down-regulated in MSC-5H-FC and T-5H-FC cells including PPARγ and C/EBPα **(Fig. 5A-**

B). RT-qPCR analysis confirmed the altered expression of these master adipogenic transcription factors **(Fig. 5B)**. The expression of the PPARγ isoform that most efficiently induces terminal adipogenic differentiation (PPARγ-2) was mainly unaffected by the expression of FC or by oncogenic cooperating mutations **(Fig. 5B)**. Nevertheless, the level of the total PPARγ mRNA (isoforms 1 and 2) increased in MSC-5H and T-5H cells, suggesting that introduction of the oncogenic mutations has an impact on the PPARγ-1 isoform, which seems to play a role earlier in adipogenesis [35] **(Fig 5A-C)**. On the other hand, the expression of C/EBPα was down-regulated in MSC-5H and T-5H **(Fig. 5B).** Thus, accumulation of the oncogenic hits appears to initially predispose the cells to a process of adipogenic differentiation, as suggested by the up-regulation of the adipogenic positive regulators PPARγ-total/ PPARγ-1, MYB or BMP2/4. However, adipogenic differentiation seems blocked at a later step, as suggested by the down-regulation of late adipogenic positive regulators such as C/EBPα, USF1, KLF2 and STAT5, and the up-regulation of TFAP2A and CHOP which function as repressors of C/EBPα **(Fig. 5C).** In order to validate this, we compared the GEP of the MSC-0H-FC, MSC-5H-FC and T-5H-FC with the GEP produced by Sekiya *et al*. [36] from different adipogenic stages in hMSCs. We found that most of the genes reported by Sekiya *et al*. [36] to be up-regulated during the earlier phases of hMSC adipogenesis, and significantly modulated in the FC-expressing cells, were also up-regulated in our MSC-0H-FC, MSC-5H-FC and T-5H-FC cells. Conversely, those genes reported by Sekiya *et al*. [36] to be up-regulated later in adipogenesis were down-regulated in our FC-expressing cells, **(Fig. 5D)**, suggesting that FC/oncogenic hits impede late/terminal rather than early adipogenic differentiation.

Gene expression analysis identifies specific signaling pathways affected by FC expression and the oncogenic mutations (5H) in the MLS model

Many (91 out of 135, 67.4%) of the genes that were differentially expressed in MSC-0H-FC cells were also differentially regulated in both MSC-5H-FC and T-5H-FC cells **(Fig 6A)**. These 91 genes commonly regulated in MSC-0H-FC, MSC-5H-FC and T-5H-FC cells **(Table S4)** represent the contribution of FC expression to the MLS model. Similarly, the GEP of MSC-5H-FC and the corresponding *ex vivo* derived tumoral cell line T-5H-FC were very similar, sharing 78-81% differentially expressed genes **(Fig 6A)**. The list of genes commonly regulated between MSC-5H-FC and T-5H-FC (2087 genes; excluding the 91 genes also regulated in MSC-0H-FC cells), represent the contribution of the oncogenic mutations (5H) to the MLS model. The combination of the genes commonly regulated by FC (91 genes) and 5H (2087 genes) explain, at least in part, the molecular basis underlying the development of MLS *in vivo*. Pathway analysis was used to group the differentially regulated genes into canonical signaling pathways that were significantly altered by FC **(Fig. 6B)** and by the oncogenic mutations (5H) **(Fig. 6C).** As expected, the canonical signaling pathways that were altered in the MLS model (MSC-5H-FC/T-5H-FC) were a combination of those signaling pathways independently regulated by FC and by 5H. Importantly, three signaling pathways (AHR-, IL-17- and VDR/RXR-mediated pathways) were commonly altered by both FC and by the oncogenic mutations (5H) **(Fig 6D)**.

DISCUSSION

Sarcomas are generally studied using primary patient samples in which full transformation events have already occurred and therefore, the mechanisms of transformation are not amenable to analysis. Hence, there exists the need to establish *bona fide* models to recapitulate sarcomagenesis *in vitro* and *in vivo*. Mounting evidence indicates that MSCs may represent the putative target cell of origin for a variety of human sarcomas, linking MSCs and cancer and encouraging the development of hMSC-based sarcoma models by targeting hMSC with the appropriate oncogenic events. Such models, like the one presented here, would improve our understanding of the mechanisms governing sarcomagenesis, eventually facilitating the testing of specific therapies directed against the sarcoma-initiating cell. In this regard, the analysis of the transcriptional profile in the collection of gradually transformed hMSCs used in the present study identified several up-regulated enzymes that could represent putative novel anti-sarcoma targets [37].

Previous attempts to reproduce human sarcomas by expressing fusion genes in hMSCs have been able to partially mimic the transcriptional expression pattern of several types of sarcomas [13, 14] but failed to transform hMSCs. We previously showed that the expression of FC in transformed leiomyosarcoma-forming p53-deficient mASCs [20] was able to redirect the tumor phenotype towards the formation of liposarcoma [9]. However, in the human setting, the expression of FC failed to transform either wt or p53-deficient hASCs [9]. We thus hypothesized that cooperating mutations are needed to transform hMSCs, so that the expression of FC together with cooperating oncogenic hits could result in liposarcoma formation similar to that reported in mASCs [9]. Here, we harnessed an available collection of sequentially mutated hMSCs ranging from MSC-0H (no oncogenic hits) to fully transformed MSC-5H (targeted with 5 oncogenic hits: p53 deficiency, Rb deficiency, hTERT expression, C-MYC stabilization and H-RAS^{V12} mutation) [21] to address

whether expression of FC in hMSCs harboring different oncogenic insults cooperates to develop a *bona fide* hMSC-based model reproducing the MLS phenotype. This hypothesis is further supported by previous studies demonstrating: (i) the acquisition of a liposarcoma phenotype upon expression of FC in a fibrosarcoma cell line [38]; (ii) the progressive accumulation of these oncogenic hits induces a gradual global hypomethylation (a hallmark of cancer) of hMSCs [39]; (iii) immortalized/transformed hMSCs harbor oncogenic mutations in genes related to relevant signaling pathways altered in liposarcoma-forming FC-expressing $p53^{-/-}$ mMSCs but not in non-transformed equivalent hMSCs [9], indicating that the introduction of these oncogenic mutations may cooperate with FC to trigger liposarcoma development from hMSCs (these pathways include p53; Wnt and PDGF signaling, associated with c-myc stabilization; and PTEN, PI3K/AKT, G-coupled receptors and FGF signaling pathways, linked to H-RAS activation); and (iv) although there are not many recurrent alterations found in human MLS, apart from the translocation encoding FC, the oncogenic targets mutated in these hMSCs or related signaling pathways are among the most relevant alterations previously described in human MLS. Thus, frequent alterations have been reported in p53, Rb and in $p16^{INK4a}$/$p14^{ARF}$ (involved in Rb regulation) in MLS tumors [30, 40]. Moreover, abnormal expression of G1 phase cell cycle proteins [32] including CDK2, which bind to FC and CHOP [41], has been reported in MLS tumors. Additionally, a p53 null background was needed for the development of a recently reported mouse model of MLS where FC was expressed by the mesoderm-specific Prx1 promoter [6], suggesting that FC synergizes with p53 in the formation of MLS. Furthermore, genome analysis of STS patients have identified a gain in chromosome 8, where the MYC gene is located, as the most common copy-number variation in MLS [33]. Point mutations in PIK3CA (associated with AKT activation) and KIT, which constitute important downstream signaling pathways for RAS oncogenic signals [42], have also been found in 18% and 4.8% of MLS cases respectively [33].

The differences of FC expression observed between the different MSCs are probably due to the lower lentiviral transduction efficiency achieved in primary hMSCs as compared to transformed cells [43]. Nevertheless, experimentally-induced FC expression is within the expression range observed in human MLS samples. The fact that MSC-3H-FC did not form tumors, indicates that the expression of appropriate levels of FC in BM-hMSCs (lacking functional p53 and Rb and expressing hTERT), is not enough to achieve tumoral transformation, in line with previous reports where FC or other sarcoma-related fusion genes are expressed in non-transformed hASCs or BM-hMSCs [9, 13, 14]. Nevertheless, we cannot discard that higher levels of FC expression or alternative oncogenic lesions could facilitate the MLS development.

The expression of FC fully transforms immortalized -non-transformed- MSC-4H cells (p53 and Rb deficiency, hTERT overexpresion and c-myc stabilization) giving rise to *in vivo* tumors resembling MLS. Furthermore, FC expression was able to redirect the tumor phenotype of the MSC-5H cells (MSC-4H plus H-RAS^{V12}) from UPSC towards MLS. This MLS phenotype could be reproduced upon serial transplantation, suggesting the existence of MLS-propagating cells. The ability of FC to redirect tumor genesis/phenotype from a UPSC to MLS indicates that this fusion oncogene has an instructive role in lineage/tissue commitment during transformation. The development of MLS tumors from MSC-4H-FC cells indicates that H-RAS^{V12} is not necessary for the development of the MLS phenotype, but that it shortens tumor latency. To the best of our knowledge, this is the first human model of sarcomagenesis resulting from the expression of a fusion oncogene in hMSCs, and constitutes a proof-of-concept to employ the same strategy to model other types of fusion gene-associated human sarcomas.

In line with previous reports, the expression of FC in MSC-0H cells largely prevented the activation of the master adipogenic factors PPARγ and CEBPα [19], resulting in a partial inhibition of the adipogenic differentiation. Similarly, the oncogenic mutations introduced in MSC-3H, MSC-4H and

MSC-5H cells largely impaired adipogenesis of hMSCs. The oncogenic mutations introduced in MSCs appear to display opposing effects on the adipogenic differentiation. For example, p53 and Rb inhibit adipogenic differentiation through repression of PPARγ [35, 44] suggesting that the deficiency of p53 and/or Rb in MSCs favours adipogenesis [44, 45]. Conversely, c-myc inhibits terminal adipocyte differentiation by suppressing PPARγ and CEBPα [46]. The introduction of oncogenic H-RAS^{V12} in MSC-5H cells almost completely blocks adipogenesis of hMSCs. This observation is supported by the potent effect of RAS^{V12} in the blockage of lipid accumulation and repression of adipocyte gene expression [47]. According to this, GEP analysis indicates that the pro-adipogenic (p53 and Rb deficiency) and anti-adipogenic (c-myc and RAS^{v-12}) cooperating mutations strongly alter the adipogenic differentiation process by inducing both positive (upregulation of PPARγ-total, c-myb, BMPs or KLF5 and downregulation of FOXO1) and negative (upregulation of GATA2/3, REL-A, TFAP2A or CHOP and downregulation of CEBPα, USF1 or STAT5A) regulators of adipogenesis. Most likely, these stimulatory/inhibitory adipogenic effects of the oncogenic mutations cooperate with FC expression in the development of MLS. This is supported by the Prx1-FC mouse model of MLS in which MSCs were committed to adipocytic differentiation but unable to terminally differentiate [6]. Also, the comparison of our GEP (MSC-5H-FC and T-5H-FC) with the genes reported by Sekiya *et al* [36] to be up-regulated during hMSCs adipogenic differentiation revealed that there is a positive correlation at earlier time points but a negative correlation at later phases. These findings suggest that the combination of FC and the oncogenic hits impede late/terminal rather than early adipogenic differentiation.

Our GEP studies revealed that IL-6 signaling is the most significantly altered pathway upon FC expression in MSCs. Accordingly, in keeping with this observation, it was previously reported that IL-6 is up-regulated in fibrosarcoma cell lines with ectopic expression of FC [48], and that IL-6 expression appears to be necessary and sufficient to enhance MSC proliferation, to inhibit MSC

apoptosis, and to prevent adipogenic and chondrogenic differentiation [49]. In addition, we found that other signaling pathways known to be involved in the modulation of adipogenesis were also altered following FC expression in our MSCs including PPAR signaling [35], VDR/RXR activation [50], NFkB [51], IL-17 [52] and aryl hydrocarbon receptor (AHR) activation [53]. On the other hand, our GEP analysis revealed that DNA damage response, cell cycle control, and pathways controlling cell fate, proliferation and differentiation (such as WNT/β-catenin, cAMP, G-coupled receptor, protein kinase A, PTEN signaling) are the pathways most significantly regulated by the introduction of oncogenic mutations (5H) in MSCs.

CONCLUSION

In summary, we have developed and characterized the first human stem cell-based model that reproduces a sarcoma phenotype upon the expression of a sarcoma-associated fusion oncogene in hMSCs. In this model of MLS, FC appears to trigger a lineage instructive role, and cooperates with oncogenic hits to block the adipogenic differentiation potential of hMSCs. We envision that this model will facilitate the *in vivo* testing of novel small-molecules directed against liposarcoma-initiating cells, and paves the way for modeling subsequent fusion gene-driven human sarcomas.

ACKNOWLEDGMENTS

We thank the Andalusian Platform of Bioinformatics (PAB; University of Málaga) for providing access to IPA software and Dr. Patrick Aebischer for the pLVUHshp53 plasmid. This work was supported by the Instituto de Salud Carlos III/Fondos FEDER (PI10/00449 to P.M, CP11/00024 to R.Ro, Tercel (RD12/0019/0006) and RTICC (RD12/0036/0015)), the Junta de Andalucía/FEDER (P08-CTS-3678 to P.M), the Spanish Association Against Cancer (Junta Provincial de Albacete-CI110023 to P.M and Junta Provincial de Granada to R.Ro), Grupo Español de Investigación en Sarcomas (beca J.M. Buesa-2012 to R. Ro), Health Canada (H4084-112281 to P.M, R.Ro, and M.R-M), Health Canada's Genomics Research and Development Initiative (to M.R-M, C.Y and A.W) and Obra Social Cajastur-IUOPA. R.Ro is supported by the Miguel Servet program of the ISCIII/FEDER. R.Ru was supported by a fellowship of the ISCIII/FEDER. P.M is an ICREA Research Professor supported by the Generalitat of Catalunya.

Conflict of interest disclosures: The authors reported no potential conflicts of interest.

REFERENCES

1. Garcia-Castro J, Trigueros C, Madrenas J*, et al.* Mesenchymal stem cells and their use as cell replacement therapy and disease modelling tool. *J Cell Mol Med* 2008;**12:**2552-2565.
2. Rodriguez R, Garcia-Castro J, Trigueros C*, et al.* Multipotent mesenchymal stromal cells: clinical applications and cancer modeling. *Adv Exp Med Biol* 2012;**741:**187-205.
3. Rodriguez R, Rubio R, Menendez P. Modeling sarcomagenesis using multipotent mesenchymal stem cells. *Cell Res* 2012;**22:**62-67.
4. Riggi N, Cironi L, Provero P*, et al.* Development of Ewing's sarcoma from primary bone marrow-derived mesenchymal progenitor cells. *Cancer Res* 2005;**65:**11459-11468.
5. Lin PP, Pandey MK, Jin F*, et al.* EWS-FLI1 induces developmental abnormalities and accelerates sarcoma formation in a transgenic mouse model. *Cancer Res* 2008;**68:**8968-8975.
6. Charytonowicz E, Terry M, Coakley K*, et al.* PPARgamma agonists enhance ET-743-induced adipogenic differentiation in a transgenic mouse model of myxoid round cell liposarcoma. *J Clin Invest* 2012;**122:**886-898.
7. Perez-Losada J, Pintado B, Gutierrez-Adan A*, et al.* The chimeric FUS/TLS-CHOP fusion protein specifically induces liposarcomas in transgenic mice. *Oncogene* 2000;**19:**2413-2422.
8. Riggi N, Cironi L, Provero P*, et al.* Expression of the FUS-CHOP fusion protein in primary mesenchymal progenitor cells gives rise to a model of myxoid liposarcoma. *Cancer Res* 2006;**66:**7016-7023.
9. Rodriguez R, Rubio R, Gutierrez-Aranda I*, et al.* FUS-CHOP fusion protein expression coupled to p53 deficiency induces liposarcoma in mouse but not in human adipose-derived mesenchymal stem/stromal cells. *Stem Cells* 2011;**29:**179-192.
10. Ren YX, Finckenstein FG, Abdueva DA*, et al.* Mouse mesenchymal stem cells expressing PAX-FKHR form alveolar rhabdomyosarcomas by cooperating with secondary mutations. *Cancer Res* 2008;**68:**6587-6597.
11. Keller C, Arenkiel BR, Coffin CM*, et al.* Alveolar rhabdomyosarcomas in conditional Pax3:Fkhr mice: cooperativity of Ink4a/ARF and Trp53 loss of function. *Genes Dev* 2004;**18:**2614-2626.
12. Haldar M, Hancock JD, Coffin CM*, et al.* A conditional mouse model of synovial sarcoma: insights into a myogenic origin. *Cancer Cell* 2007;**11:**375-388.
13. Riggi N, Suva ML, Suva D*, et al.* EWS-FLI-1 expression triggers a Ewing's sarcoma initiation program in primary human mesenchymal stem cells. *Cancer Res* 2008;**68:**2176-2185.
14. Cironi L, Provero P, Riggi N*, et al.* Epigenetic features of human mesenchymal stem cells determine their permissiveness for induction of relevant transcriptional changes by SYT-SSX1. *PLoS One* 2009;**4:**e7904.
15. Fletcher O, Houlston RS. Architecture of inherited susceptibility to common cancer. *Nat Rev Cancer* 2010;**10:**353-361.
16. Singer S, Nielsen T, Antonescu C. Molecular Biology of Soft Tissue Sarcoma. In: DeVita V, Lawrence T, Rosenberg S, editors. *Cancer: Principles & Practice of Oncology* 9ed. Philadelphia: Wolters; 2011. p. 1522 - 1532.
17. Sanchez-Garcia I, Rabbitts TH. Transcriptional activation by TAL1 and FUS-CHOP proteins expressed in acute malignancies as a result of chromosomal abnormalities. *Proc Natl Acad Sci U S A* 1994;**91:**7869-7873.
18. Ron D, Habener JF. CHOP, a novel developmentally regulated nuclear protein that dimerizes with transcription factors C/EBP and LAP and functions as a dominant-negative inhibitor of gene transcription. *Genes Dev* 1992;**6:**439-453.
19. Perez-Mancera PA, Bermejo-Rodriguez C, Sanchez-Martin M*, et al.* FUS-DDIT3 prevents the development of adipocytic precursors in liposarcoma by repressing PPARgamma and C/EBPalpha and activating eIF4E. *PLoS One* 2008;**3:**e2569.

20. Rubio R, Garcia-Castro J, Gutierrez-Aranda I, *et al.* Deficiency in p53 but not retinoblastoma induces the transformation of mesenchymal stem cells in vitro and initiates leiomyosarcoma in vivo. *Cancer Res* 2010;**70:**4185-4194.
21. Funes JM, Quintero M, Henderson S, *et al.* Transformation of human mesenchymal stem cells increases their dependency on oxidative phosphorylation for energy production. *Proc Natl Acad Sci U S A* 2007;**104:**6223-6228.
22. Szulc J, Wiznerowicz M, Sauvain MO, *et al.* A versatile tool for conditional gene expression and knockdown. *Nat Methods* 2006;**3:**109-116.
23. Menendez P, Catalina P, Rodriguez R, *et al.* Bone marrow mesenchymal stem cells from infants with MLL-AF4+ acute leukemia harbor and express the MLL-AF4 fusion gene. *J Exp Med* 2009;**206:**3131-3141.
24. Rodriguez R, Rubio R, Masip M, *et al.* Loss of p53 induces tumorigenesis in p21-deficient mesenchymal stem cells. *Neoplasia* 2009;**11:**397-407.
25. Rubio R, Gutierrez-Aranda I, Saez-Castillo AI, *et al.* The differentiation stage of p53-Rb-deficient bone marrow mesenchymal stem cells imposes the phenotype of in vivo sarcoma development. *Oncogene* 2012.
26. Rodriguez R, Gagou ME, Meuth M. Apoptosis induced by replication inhibitors in Chk1-depleted cells is dependent upon the helicase cofactor Cdc45. *Cell Death Differ* 2008;**15:**889-898.
27. Bueno C, Montes R, Melen GJ, *et al.* A human ESC model for MLL-AF4 leukemic fusion gene reveals an impaired early hematopoietic-endothelial specification. *Cell Res* 2012;**22:**986-1002.
28. Gutierrez-Aranda I, Ramos-Mejia V, Bueno C, *et al.* Human induced pluripotent stem cells develop teratoma more efficiently and faster than human embryonic stem cells regardless the site of injection. *Stem Cells* 2010;**28:**1568-1570.
29. Hashimoto H, Daimaru Y, Enjoji M. S-100 protein distribution in liposarcoma. An immunoperoxidase study with special reference to the distinction of liposarcoma from myxoid malignant fibrous histiocytoma. *Virchows Arch A Pathol Anat Histopathol* 1984;**405:**1-10.
30. Dei Tos AP, Piccinin S, Doglioni C, *et al.* Molecular aberrations of the G1-S checkpoint in myxoid and round cell liposarcoma. *Am J Pathol* 1997;**151:**1531-1539.
31. Negri T, Virdis E, Brich S, *et al.* Functional mapping of receptor tyrosine kinases in myxoid liposarcoma. *Clin Cancer Res* 2010;**16:**3581-3593.
32. Olofsson A, Willen H, Goransson M, *et al.* Abnormal expression of cell cycle regulators in FUS-CHOP carrying liposarcomas. *Int J Oncol* 2004;**25:**1349-1355.
33. Barretina J, Taylor BS, Banerji S, *et al.* Subtype-specific genomic alterations define new targets for soft-tissue sarcoma therapy. *Nat Genet* 2010;**42:**715-721.
34. Matushansky I, Hernando E, Socci ND, *et al.* A developmental model of sarcomagenesis defines a differentiation-based classification for liposarcomas. *Am J Pathol* 2008;**172:**1069-1080.
35. Farmer SR. Transcriptional control of adipocyte formation. *Cell Metab* 2006;**4:**263-273.
36. Sekiya I, Larson BL, Vuoristo JT, *et al.* Adipogenic differentiation of human adult stem cells from bone marrow stroma (MSCs). *J Bone Miner Res* 2004;**19:**256-264.
37. Flanagan JM, Funes JM, Henderson S, *et al.* Genomics screen in transformed stem cells reveals RNASEH2A, PPAP2C, and ADARB1 as putative anticancer drug targets. *Mol Cancer Ther* 2009;**8:**249-260.
38. Engstrom K, Willen H, Kabjorn-Gustafsson C, *et al.* The myxoid/round cell liposarcoma fusion oncogene FUS-DDIT3 and the normal DDIT3 induce a liposarcoma phenotype in transfected human fibrosarcoma cells. *Am J Pathol* 2006;**168:**1642-1653.
39. Wild L, Funes JM, Boshoff C, *et al.* In vitro transformation of mesenchymal stem cells induces gradual genomic hypomethylation. *Carcinogenesis* 2010;**31:**1854-1862.

40. Oda Y, Yamamoto H, Takahira T*, et al.* Frequent alteration of p16(INK4a)/p14(ARF) and p53 pathways in the round cell component of myxoid/round cell liposarcoma: p53 gene alterations and reduced p14(ARF) expression both correlate with poor prognosis. *J Pathol* 2005;**207:**410-421.
41. Bento C, Andersson MK, Aman P. DDIT3/CHOP and the sarcoma fusion oncoprotein FUS-DDIT3/TLS-CHOP bind cyclin-dependent kinase 2. *BMC Cell Biol* 2009;**10:**89.
42. Liu Y, Wang DL, Chen S*, et al.* Oncogene Ras/phosphatidylinositol 3-kinase signaling targets histone H3 acetylation at lysine 56. *J Biol Chem* 2012;**287:**41469-41480.
43. Lin P, Correa D, Lin Y*, et al.* Polybrene inhibits human mesenchymal stem cell proliferation during lentiviral transduction. *PLoS One* 2011;**6:**e23891.
44. Molchadsky A, Rivlin N, Brosh R*, et al.* p53 is balancing development, differentiation and de-differentiation to assure cancer prevention. *Carcinogenesis* 2010;**31:**1501-1508.
45. Calo E, Quintero-Estades JA, Danielian PS*, et al.* Rb regulates fate choice and lineage commitment in vivo. *Nature* 2010;**466:**1110-1114.
46. Heath VJ, Gillespie DA, Crouch DH. Inhibition of the terminal stages of adipocyte differentiation by cMyc. *Exp Cell Res* 2000;**254:**91-98.
47. Murholm M, Dixen K, Hansen JB. Ras signalling regulates differentiation and UCP1 expression in models of brown adipogenesis. *Biochim Biophys Acta* 2010;**1800:**619-627.
48. Goransson M, Elias E, Stahlberg A*, et al.* Myxoid liposarcoma FUS-DDIT3 fusion oncogene induces C/EBP beta-mediated interleukin 6 expression. *Int J Cancer* 2005;**115:**556-560.
49. Pricola KL, Kuhn NZ, Haleem-Smith H*, et al.* Interleukin-6 maintains bone marrow-derived mesenchymal stem cell stemness by an ERK1/2-dependent mechanism. *J Cell Biochem* 2009;**108:**577-588.
50. Wood RJ. Vitamin D and adipogenesis: new molecular insights. *Nutr Rev* 2008;**66:**40-46.
51. Takada I, Kouzmenko AP, Kato S. PPAR-gamma Signaling Crosstalk in Mesenchymal Stem Cells. *PPAR Res* 2010;**2010:**pii: 341671.
52. Zuniga LA, Shen WJ, Joyce-Shaikh B*, et al.* IL-17 regulates adipogenesis, glucose homeostasis, and obesity. *J Immunol* 2010;**185:**6947-6959.
53. Shin S, Wakabayashi N, Misra V*, et al.* NRF2 modulates aryl hydrocarbon receptor signaling: influence on adipogenesis. *Mol Cell Biol* 2007;**27:**7188-7197.

TABLES

Table 1. *In vivo* tumor formation ability.

MSC type	Tumours/Mice (penetrance)	Latency*	Histological Analysis
0H-GFP	0/4 (0%)	-	-
0H-FC	0/4 (0%)	-	-
1H-GFP	0/4 (0%)	-	-
1H-FC	0/4 (0%)	-	-
3H-GFP	0/7 (0%)	-	-
3H-FC	0/7 (0%)	-	-
4H-GFP	0/7 (0%)	-	-
4H-FC	6/7 (85%)	138±32	Myxoid liposarcoma
5H-GFP	7/7 (100%)	25±2	Undif. spindle cell sarcoma (UPCS)
5H-FC	7/7 (100%)	25±2	Myxoid liposarcoma + UPCS

(*): Mean of days (± standard deviation) needed to observe an approximate tumor volume of $1cm^3$.

FIGURE LEGENDS

Figure 1. FC expression in immortalized/transformed hMSCs initiates mixoid liposarcoma-like tumors *in vivo*. (A) Summary of the BM-hMSCs types used in this study. The oncogenic hits used are indicated. **(B)** End-point RT-PCR confirming the expression of FC at mRNA level in MSCs and human MLS samples (MLS#5 & #6; N & T: normal and tumoral samples obtained from the same patient). GAPDH was used as housekeeping gene. **(C)** Western blotting showing the expression of FC protein using an anti-GADD153/CHOP antibody. The expression of FUS was used as loading control. **(D)** RT-qPCR comparing the expression of FC in MSCs with human MLS samples (MLS#1 to #6). mRNA expression was referred to the FC levels in the MLS sample with higher expression (MLS#6: 100%). **(E-G)** Hematoxilin-eosin (H&E) staining and GFP immuno-staining detection in tumors developed from MSC-4H-FC **(E)**, MSC-5H-GFP **(F)**, and MSC-5H-FC **(G)** cells. MSC-4H-FC- and MSC-5H-FC-derived tumors display *bona fide* histological characteristics of human MLS [myxoid matrix (M); round-cell areas (R); lipoblasts (blue arrows); and plexiform vascular pattern (red arrows)]. Original magnification is indicated.

Figure 2: Immortalized FC-expressing cell lines *ex vivo*-derived from primary tumors reinitiate MLS in secondary recipients. Several cell lines were *ex vivo*-derived from primary tumors developed from MSC-5H-GFP (T-5H-GFP#1 to #3), MSC-5H-FC (T-5H-FC#1 to #3), and MSC-4H-FC (T-4H-FC#1 & #2) cells. **(A)** End-point RT-PCR confirming the expression of FC at mRNA level in MSCs and human MLS samples (MLS#5 & #6; N & T: normal and tumoral samples obtained from the same patient). GAPDH was used as housekeeping gene. **(B)** Western blotting showing the expression of FC protein in T-5H-FC and T-4H-FC cell lines. The expression of FUS was used as loading control. **(C)** RT-qPCR comparing the expression of FC in MSCs with human MLS samples (MLS#1 to #6). mRNA expression was referred to the FC levels in the MLS sample with higher expression (MLS#6: 100%). **(D)** Summary table indicating tumor incidence, latency,

and histological analysis of tumors developed upon secondary inoculation in NOD/SCID mice of the indicated cell lines. **(E-F)** H&E staining of tumors developed from the T-4H-FC **(E)** and the T-5H-FC cells **(F)**. Similar to primary tumors, second-round tumors display the main characteristic of myxoid liposarcomas [myxoid matrix (M); round-cell areas (R); lipoblasts (blue arrows); and plexiform vascular pattern (red arrows)]. **(G)** Hierarchical clustering of the gene expression data of T-5H-GFP (combination of T-5H-GFP#1 and #2) and T-5H-FC (combination of T-5H-FC#1 and #2) cell lines and the human sarcoma gene expression data set GSE 21122 [33]. T-5H-FC cells cluster closer to human primary MLS as compared to T-5H-GFP cells.

Figure 3. Adipogenic differentiation of control and FC-expressing hMSCs and tumoral cell lines. Representative images of the indicated GFP- and FC-expressing hMSCs **(A)**, and tumoral cell lines **(C)** following 14 days culture in adipogenic medium (or control medium in insets) and Oil Red staining. **(B)** Quantification of the adipogenic fold-induction relative to cells cultured in control medium (n=3; *p-value<0.05 vs MSC-0H-GFP cells).

Figure 4. FC and the accumulation of oncogenic hits cooperate to disrupt the expression of master adipogenic transcription factors. (A) RT-qPCR and **(B)** Western blotting analysis showing the induction of master adipogenic-related genes in the indicated hMSCs and tumoral cell lines after 0, 7 and 14 days in adipogenic inductive culture conditions. The expression of β-actin was used as loading control in the Western blotting experiments.

Figure 5. Gene expression analysis confirms a late/terminal blockage in adipogenic differentiation of MSC-5H-FC and T-5H-FC MLS cellular models. Genes differentially expressed (p value<0.005; expression >2-fold or down) in MSC-0H-FC, MSC-5H-FC and T-5H-FC cells as compared to MSC-0H-GFP (wild type/control cells) were analyzed using the IPA software. **(A)** List

of positive (top) and negative (bottom) regulators of adipogenesis differentially expressed between MSC-0H-FC, MSC-5H-FC and T-5H-FC *versus* MSC-0H-GFP. Grey color indicates alteration of the upstream regulators signaling without significant up- or down-regulation of their own expression. Green and red colors indicate significant down- and up-regulation, respectively, as compared to MSC-0H-GFP. The fold change values are indicated. **(B)** RT-qPCR analysis confirming the regulation of key adipogenic-related genes in the indicated hMSCs and tumoral cell lines relative to MSC-0H-GFP cells. **(C)** Cartoon depicting the activation/repressive role of altered regulators during adipogenesis. **(D)** Comparison between the genes up-regulated during the adipogenic differentiation process of hMSCs (data from Sekiya *et al*. 2004 [36]; left panel) and the genes significantly altered in MSC-0H-FC, MSC-5H-FC and T-5H-FC cells (relative to MSC-0H-GFP). Green and red colors indicate significant down- and up-regulation, respectively. The fold change values are indicated. The genes reported by Sekiya *et al* to reach maximum activation early during adipogenesis are mainly found up-regulated in FC-expressing cells whereas those genes found by Sekiya *et al* up-regulated later in adipogenesis are mainly down-regulated in FC-expressing cells.

Figure 6. Signaling pathways significantly regulated by FC and/or by the oncogenic mutations (5H) in the MSC-5H-FC and T-5H-FC MLS model. (A) Venn diagram representing the number and overlay of genes differentially expressed in MSC-0H-FC, MSC-5H-FC or T-5H-FC relative to MSC-0H-GFP cells. As many as 91 out of 135 genes (67.4%) differentially expressed in MSC-0H-FC cells were shared by both MSC-5H-FC cells and T-5H-FC tumoral cell lines. Furthermore, between 77.6-81.5% of the genes differentially expressed in MSC-5H-FC and T-5H-FC cells are common. **(B-D)** Lists of significantly ($p<0.05$) modulated canonical signaling pathways generated using IPA software with the genes annotated in Figure 6A. **(B)** Signaling pathways commonly altered in MSC-0H-FC, MSC-5H-FC and T-5H-FC cells (91 genes), identifying the

contribution of the FC expression to the development of the MLS model (red dotted line). **(C)** Signaling pathways specifically altered in both MSC-5H-FC and T-5H-FC cells (2087 genes) identifying the contribution of the oncogenic mutations (5H) to the MLS model (blue dotted line)**.** **(D)** Signaling pathways commonly regulated by the synergic contribution of FC and oncogenic mutations 5H (91+2087 genes), identifying the molecular basis underlying the development of MLS *in vivo* (purple dotted line).

A

BM-MSC	Hit#1	Target	Hit#2	Target	Hit#3	Target	Hit#4	Target	Hit#5	Target
MSC-0H										
MSC-1H	shRNA p53	p53 depletion								
MSC-3H	HPV-16 E6	p53 degradat.	HPV-16 E7	Rb family inactivat.	hTERT	human telomerase				
MSC-4H	HPV-16 E6	p53 degradat.	HPV-16 E7	Rb family inactivat.	hTERT	human telomerase	SV40 -ST	c-Myc stabilizat.		
MSC-5H	HPV-16 E6	p53 degradat.	HPV-16 E7	Rb family inactivat.	hTERT	human telomerase	SV40 -ST	c-Myc stabilizat.	RAS^{V12}	mitogenic signal

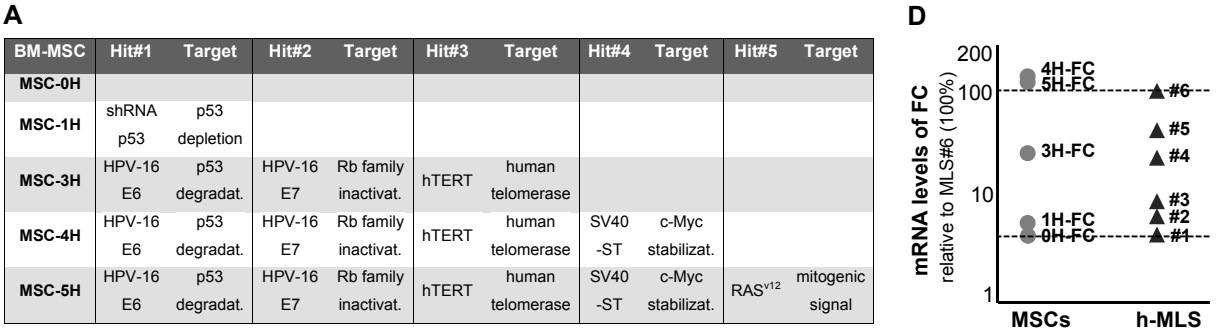

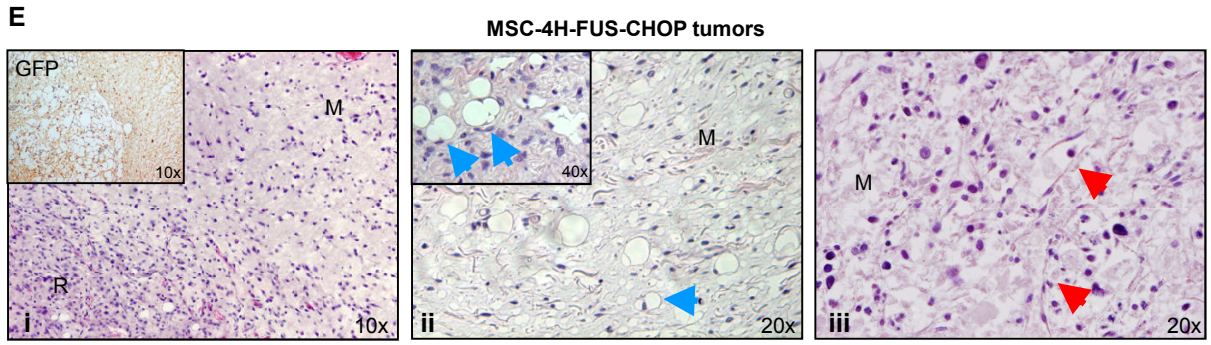

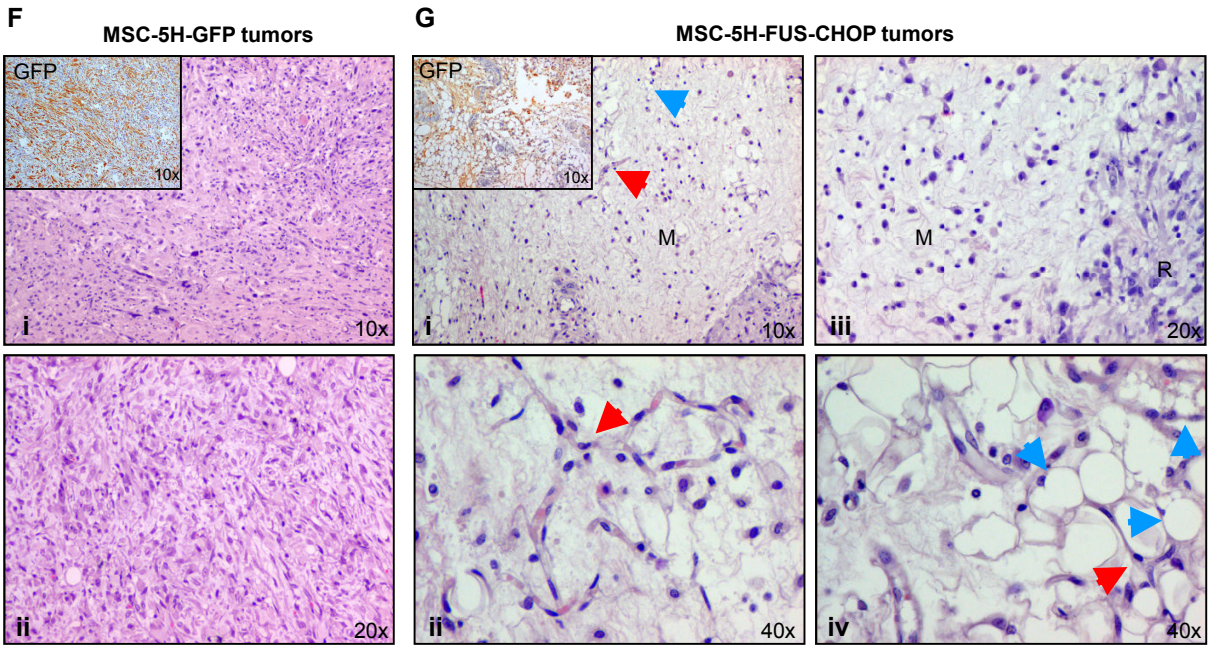

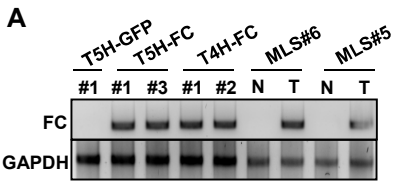

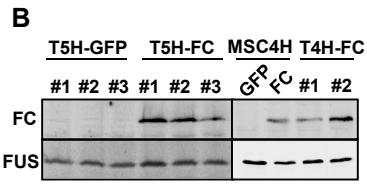

D

Tumor cell lines	Tumors /Mice	Latency	Histological Analysis
T4H-FC#2	4/4	38±5	MLS
T5H-GFP#1	5/5	15±1	UPCS
T5H-FC#1	5/5	15±1	MLS

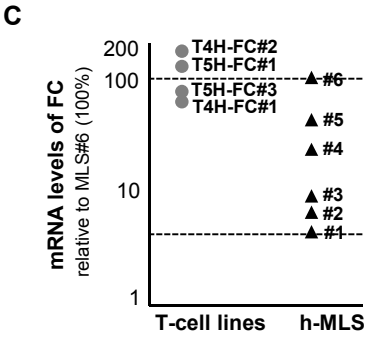

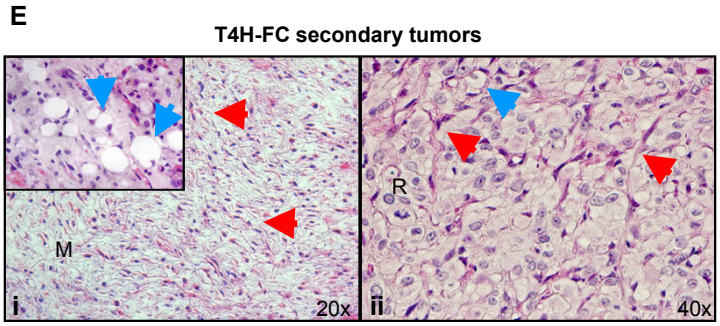

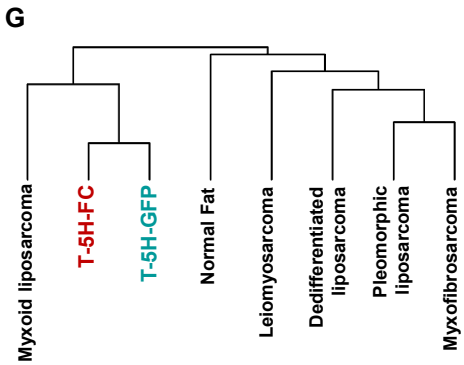

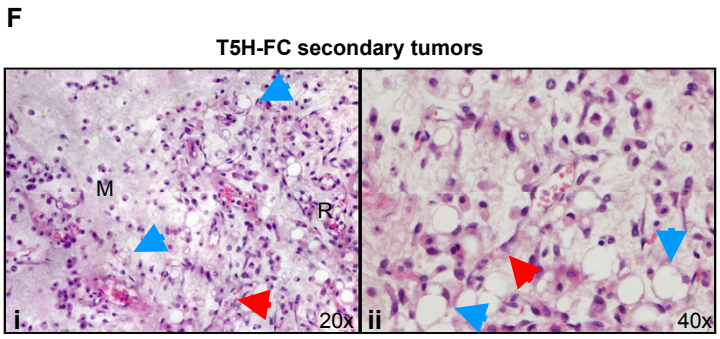

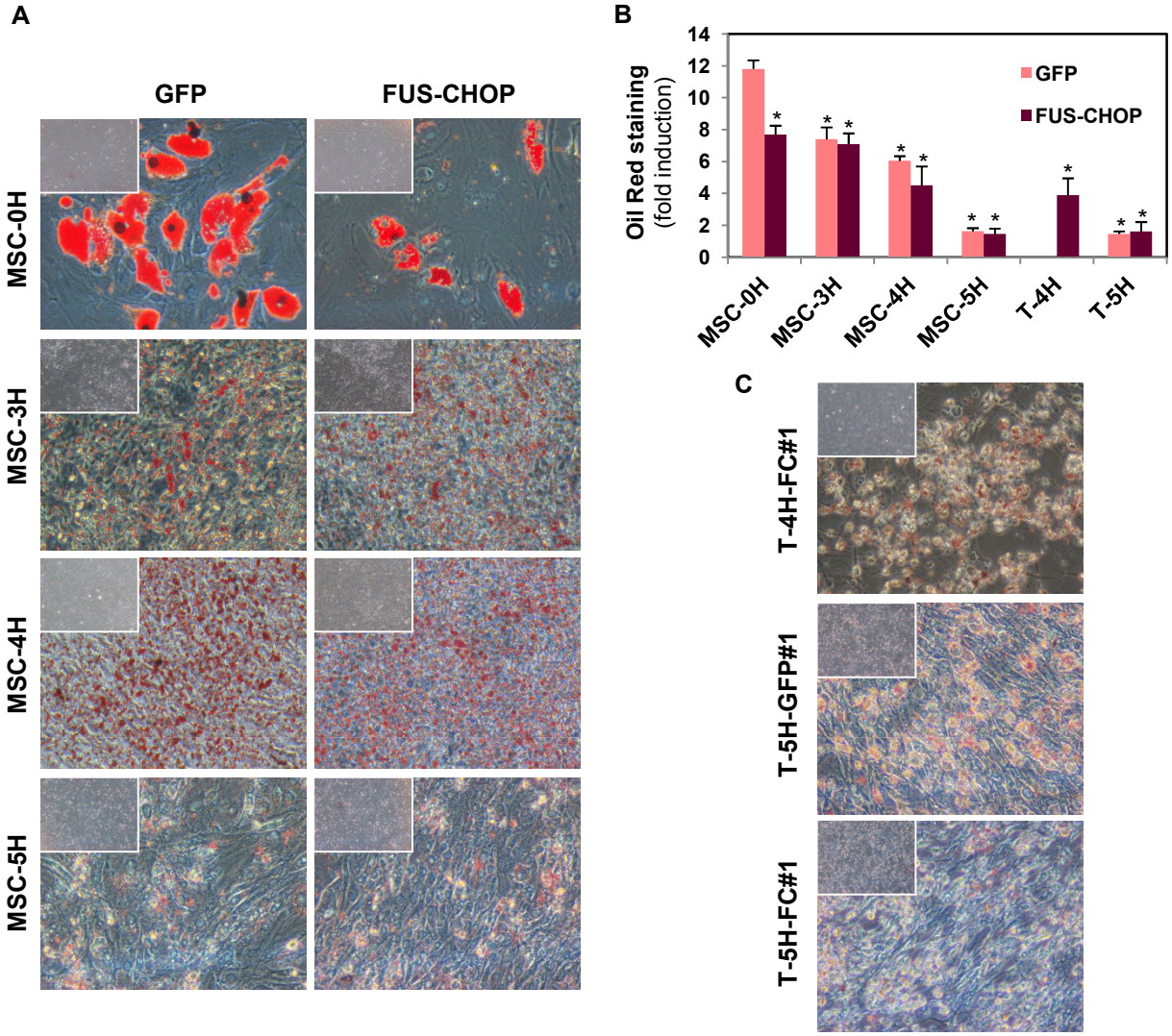
A
GFP
FUS-CHOP
MSC-0H
MSC-3H
MSC-4H
MSC-5H
B
Oil Red staining
(fold induction)
14
12
10
8
6
4
2
0
GFP
FUS-CHOP
MSC-0H
MSC-3H
MSC-4H
MSC-5H
T-4H
T-5H
C
T-4H-FC#1
T-5H-GFP#1
T-5H-FC#1

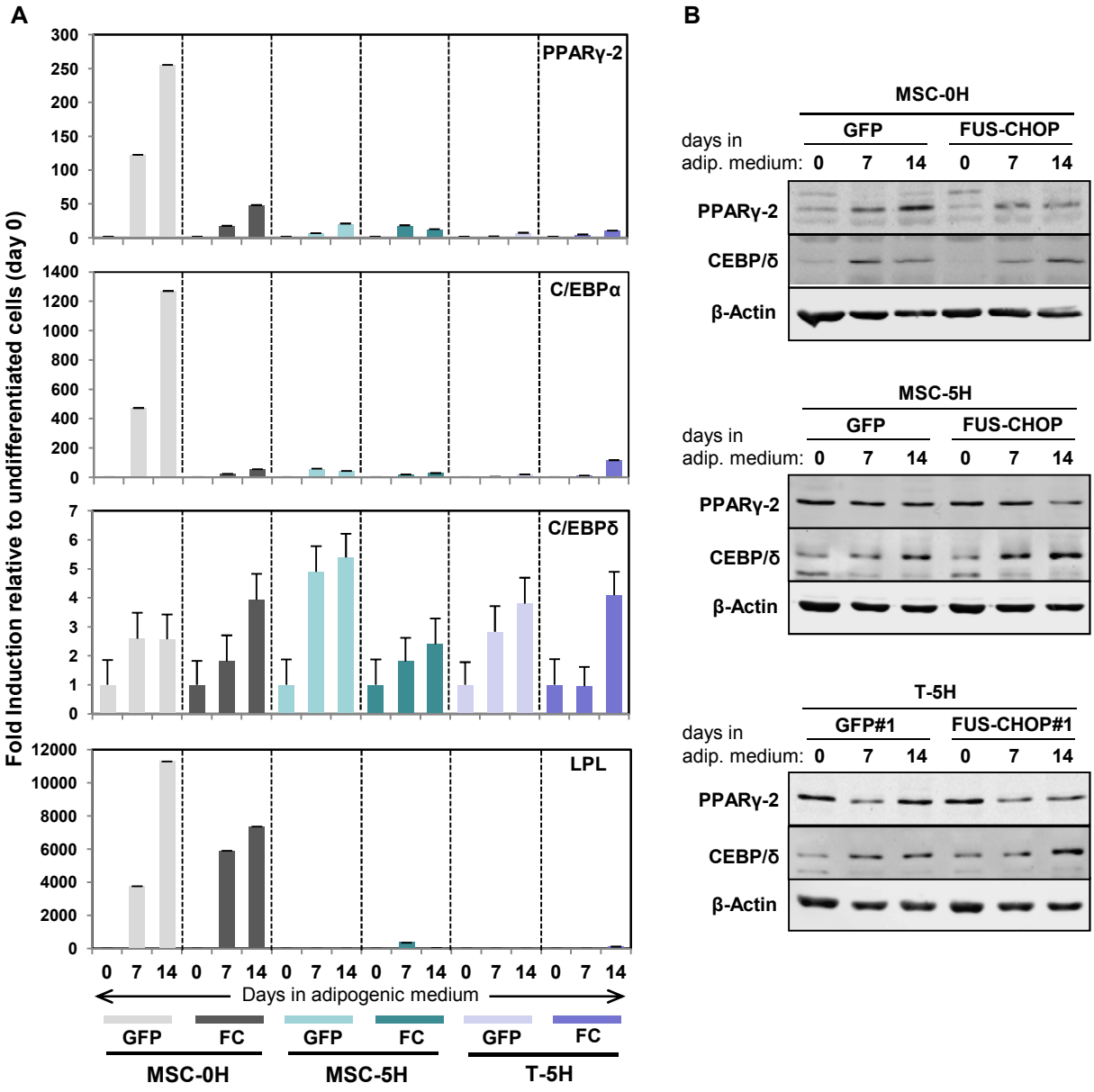
A
Fold Induction relative to undifferentiated cells (day 0)
PPARγ-2
C/EBPα
C/EBPδ
LPL
0 7 14 0 7 14 0 7 14 0 7 14 0 7 14 0 7 14
Days in adipogenic medium
GFP FC GFP FC GFP FC
MSC-0H MSC-5H T-5H
B
MSC-0H
GFP FUS-CHOP
days in adip. medium: 0 7 14 0 7 14
PPARγ-2
CEBP/δ
β-Actin
MSC-5H
GFP FUS-CHOP
days in adip. medium: 0 7 14 0 7 14
PPARγ-2
CEBP/δ
β-Actin
T-5H
GFP#1 FUS-CHOP#1
days in adip. medium: 0 7 14 0 7 14
PPARγ-2
CEBP/δ
β-Actin

A

	Molecule	Role in adipogenesis	M0H-FC	M5H-FC	T5H-FC
positive regulation	PPARγ	terminal different. effector; central role		4.26	4.42
	CEBPα	terminal different. effector; central role		-2.91	-2.6
	CEBPβ	early different. effector; central role			
	CEBPδ	early different. effector; central role			
	EGR2/KROX20	induction of CEBPβ		-2.05	
	STAT5A	dowsntream of PPARγ & CEBPα		-2.67	-2.67
	USF1	regulator of CEBPα promoter	-4.6	-3.95	-3.89
	KLF5	mediate PPARγ activation by CEBP's			2.28
	E2F1	clon expansion; induce PPARγ1/CEBPα		3.1	2.63
	MYB	enhancement of adipog. diff. in hMSCs		5.46	4.27
	BMP2	regulation of lineage commitment		2.76	3.36
	BMP4	regulation of lineage commitment			3.54
negative regulation	FOXO1	arrest of mitotic clonal expansion		-3.55	-3.46
	KLF2	repression of PPARγ promoter		-2.05	
	RUNX1T1/ETO	inhibition of CEBPβ activity		-3.15	-5.17
	TFAP2A	repression of CEBPα promoter		4.97	4.12
	GATA2	inhibition of CEBP activity		2.73	2.8
	GATA3	inhibition of CEBP activity		5.27	6.77
	DDIT3/CHOP	inhibition of CEBP activity			2.17
	E2F4	inhibition of terminal differentiation			
	RELA	increased in adipog.- inhib. of PPARγ		2.16	

C

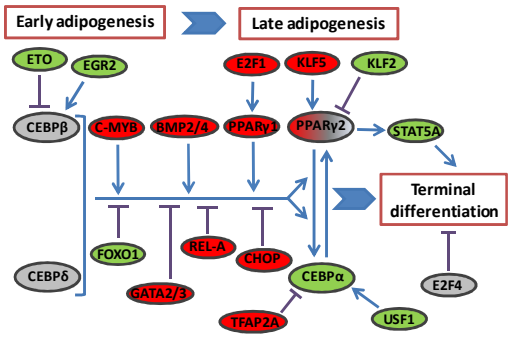

B

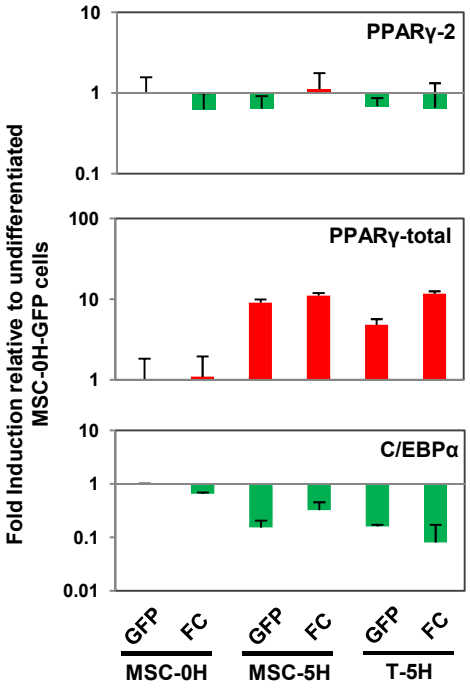

D

genes upregulated during hMSCs adipogenic differentiation						
time sequence of maximum gene expression (Sekiya et al.)				fold change in FUS-CHOP expressing cells		
day 1	day 7	day 14	day 21	M0H-FC	M5H-FC	T5H-FC
NPTX1				5.59	11.64	10.34
CXCL1					9.85	9.61
IMPA2					-2.73	-3.89
	IL8			2.36	12.69	12.02
	ACTG2			5.03	6.46	7.57
	GCHFR					3.23
	C1R				-2.98	-4.49
	GAS1				-4.11	-4.47
	MYH11				-4.76	-3.99
	IGFBP2				-6.30	-5.01
	AGT				-7.52	-7.17
	CHI3L1				-11.20	-11.10
		PPARγ			4.27	4.42
		IL18R1			2.71	3.16
		HSD11B1			2.56	
		SERPING1			-3.17	-3.67
		PTK2B			-3.57	-2.95
		FOS		-3.85	-4.00	-3.47
		IBSP			-3.52	-4.10
		IGF2				-3.96
		SAA1			-4.95	
		RBP4			-4.71	-6.36
		IGF1			-5.52	-5.59
		FGF7			-10.13	-9.01
			CHI3L2	3.52	3.68	4.12
			MVD		2.08	2.08
			CDKN1C	-2.08	-2.08	
			PPL		-2.51	
			CEBPα		-2.91	-2.60
			FOXO1		-3.55	-3.46
			CRLF1		-4.42	-4.46
			COL11A1		-5.67	-5.67
			COMP		-10.08	-10.21

A

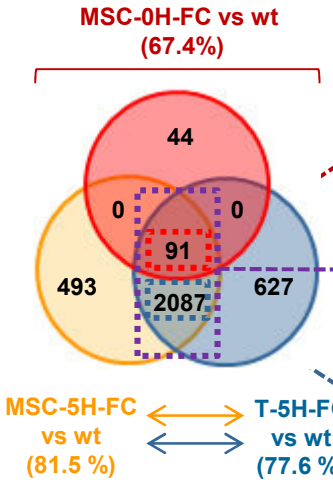

B

Contribution of FC	
Canonical Pathways	p-value
IL-6 Signaling	1.55E-05
IL-10 Signaling	2.00E-05
Role of IL-17A	2.63E-05
PPAR Signaling	7.24E-05
Cdc42 Signaling	3.55E-04
HMGB1 Signaling	8.91E-04
p38 MAPK Signaling	1.78E-03
OX40 Signaling Pathway	2.40E-03
VDR/RXR Activation	2.75E-03
Aryl Hydroc. Recep. Sign.	4.37E-03
ErbB Signaling	7.08E-03
TREM signalling	2.82E-02
RhoGDI Signaling	4.17E-02
NF-κB Signaling	4.17E-02

C

Contribution of oncogenic mutations	
Canonical Pathways	p-value
DNA Damage Response	4.07E-07
Cell Cycle Control	1.95E-05
GADD45 Signaling	4.57E-04
cAMP-mediated signaling	1.35E-03
Wnt/β-catenin Signaling	2.29E-03
G-Prot. Coup. Recep. Sign.	2.63E-03
Coagulation System	3.80E-03
Aryl Hydroc. Recep. Sign.	3.98E-03
Protein Kinase A Sign.	1.07E-02
IL-8 Signaling	1.48E-02
VDR/RXR Activation	2.04E-02
Role of IL-17A	3.80E-02
IL-4 Signaling	3.98E-02
PTEN Signaling	4.01E-02

D

MLS model	
Canonical Pathways	p-value
DNA Damage Response	8.71E-07
Cell Cycle Control	3.09E-05
Aryl Hydroc. Recep. Sign.	1.15E-03
GADD45 Signaling	1.78E-03
G-Prot. Coup. Recep. Sign.	1.86E-03
cAMP-mediated signaling	2.69E-03
Role of IL-17A	3.24E-03
VDR/RXR Activation	5.01E-03
Wnt/β-catenin Signaling	5.13E-03
Coagulation System	5.50E-03
IL-8 Signaling	6.76E-03
PPAR Signaling	1.26E-02
Protein Kinase A Sign.	1.48E-02
IL-4 Signaling	1.51E-02
p38 MAPK Signaling	1.66E-02
IL-6 Signaling	2.34E-02
NF-κB Signaling	2.95E-02
TREM signalling	3.63E-02
HMGB1 Signaling	4.57E-02
PTEN Signaling	4.68E-02

Rodriguez et al. **Supplementary Figure 1**

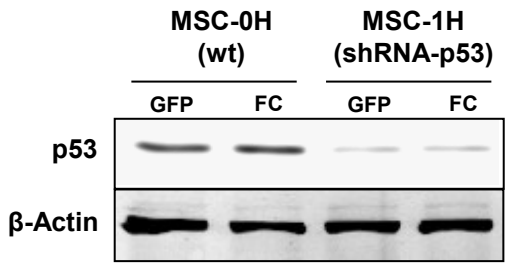

Supplementary Figure 1. Depletion of p53 by specific shRNA in MSC-1H-GFP and MSC-1H-FC cells. Western blotting showing the level of total p53 before (MSC-0H-GFP and MSC-0H-FC) and after (MSC-1H-GFP and MSC-1H-FC) the transduction with lentiviral particles expressing shRNA specific for p53. β- actin was used as loading control.

Rodriguez et al. **Supplementary Figure 2**

A

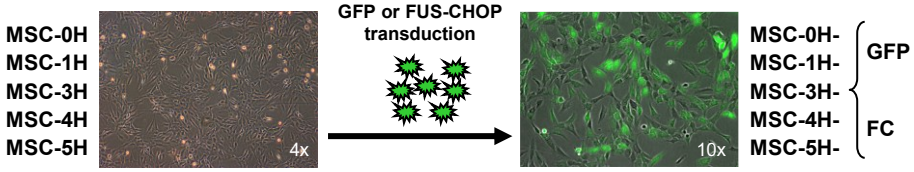

B

Transduction efficiency*

BM-hMSC	pRRL-GFP	pRRL-FUSCHOP-GFP
MSC-0H (wild type)	48.2	51.2
MSC-1H	76.6	93.1
MSCs-3H	72.5	95.5
MSCs-4H	80.1	96.0
MSCs-5H	69.5	92.0

* % of GFP+ cells as shown by flow cytometry

Supplementary Figure 2. Ectopic expression of FC in mutated hMSCs. (A) Scheme of the lentiviral transduction of MSC-0H, MSC-1H, MSC-3H, MSC-4H and MSC-5H with GFP- or GFP/FC-expressing lentivectors. **(B)** Transduction efficiencies measured as the percentage of GFP expressing cells after lentiviral transduction.

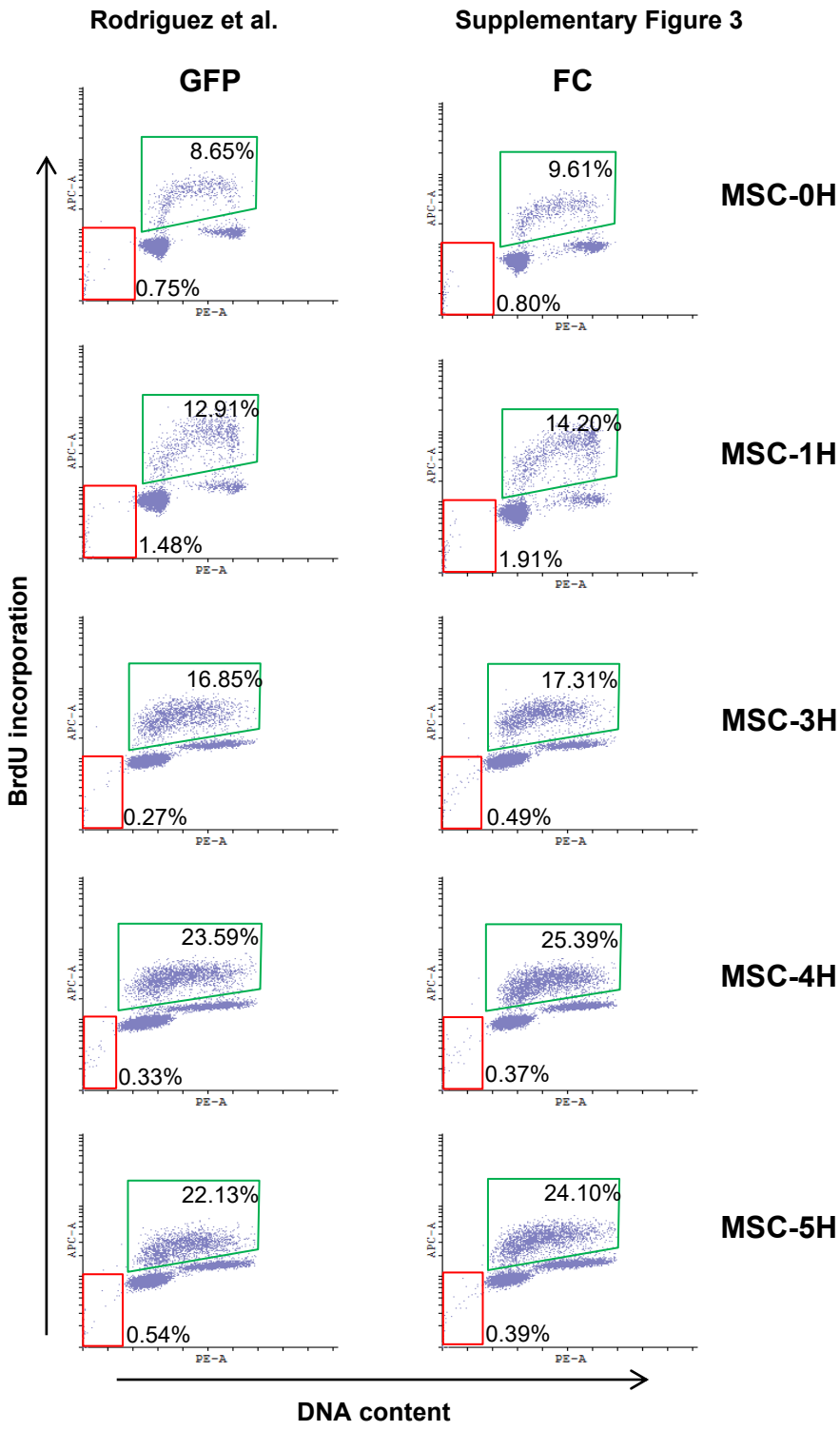

Supplementary Figure 3: Cell cycle analysis of the different MSCs. The indicated MSCs were labelled with BrdU for 30 min before being fixed with 70% ice-cold ethanol. Then cells were analyzed by flow cytometry for BrdU incorporation and DNA content (propidium iodide uptake) as previously described (Rene Rodriguez et al. Clinical Cancer Research. 2008; 14(17): p.5476-5483). Green gates (BrdU positive cells) contain the fraction of cells in S-phase. Red gates enclose apoptotic/death cells displaying the typical Sub-G_1 DNA content. No significant changes were observed in proliferation (% of cells in S-Phase) or apoptosis (% of cells presenting Sub- G_1 population) between control (GFP) and FC-expressing MSCs.

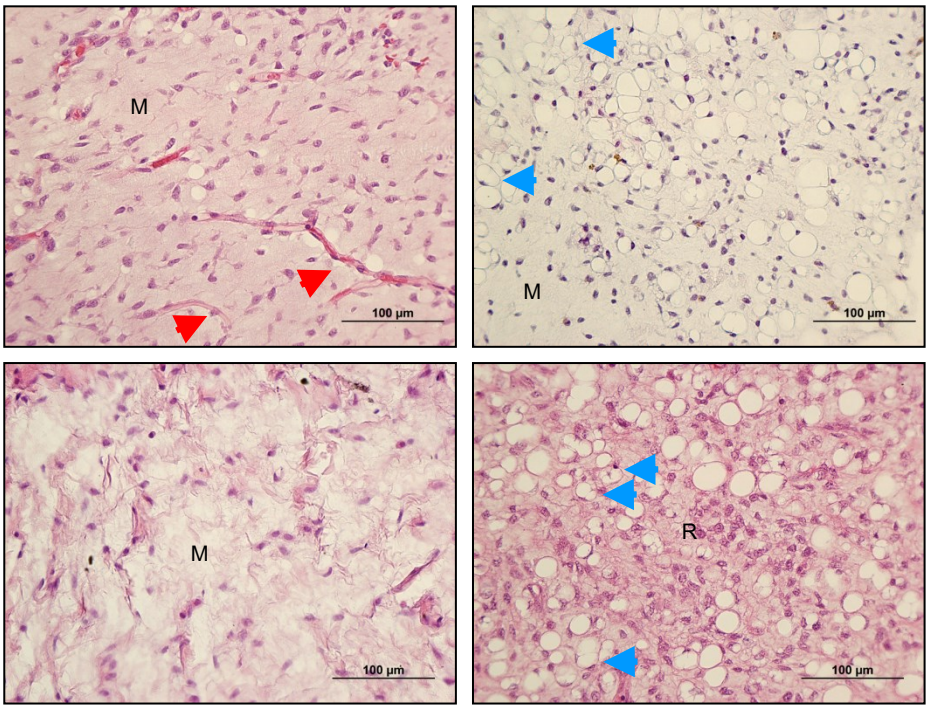

Supplementary Figure 4. Human MLS. Representative H&E staining of a human MLS sample. The presence of myxoid matrix (M), round-cell areas (R), lipoblasts (blue arrows) and plexiform vascular pattern (red arrows) is indicated.

Rodriguez et al. **Supplementary Figure 5**

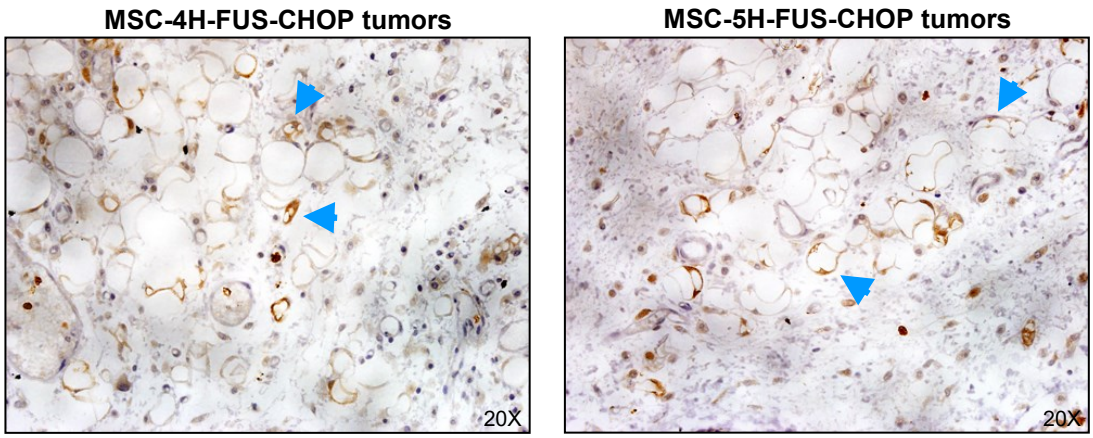

Supplementary Figure 5. Expression of S-100 in experimentally induced MLS. S-100 immuno-staining detection in tumors developed from MSC-4H-FC and MSC-5H-FC cells. Many univacuolated and multivacuolated lipoblasts (blue arrows) as well as other round and spindle cells stain positive for S-100.

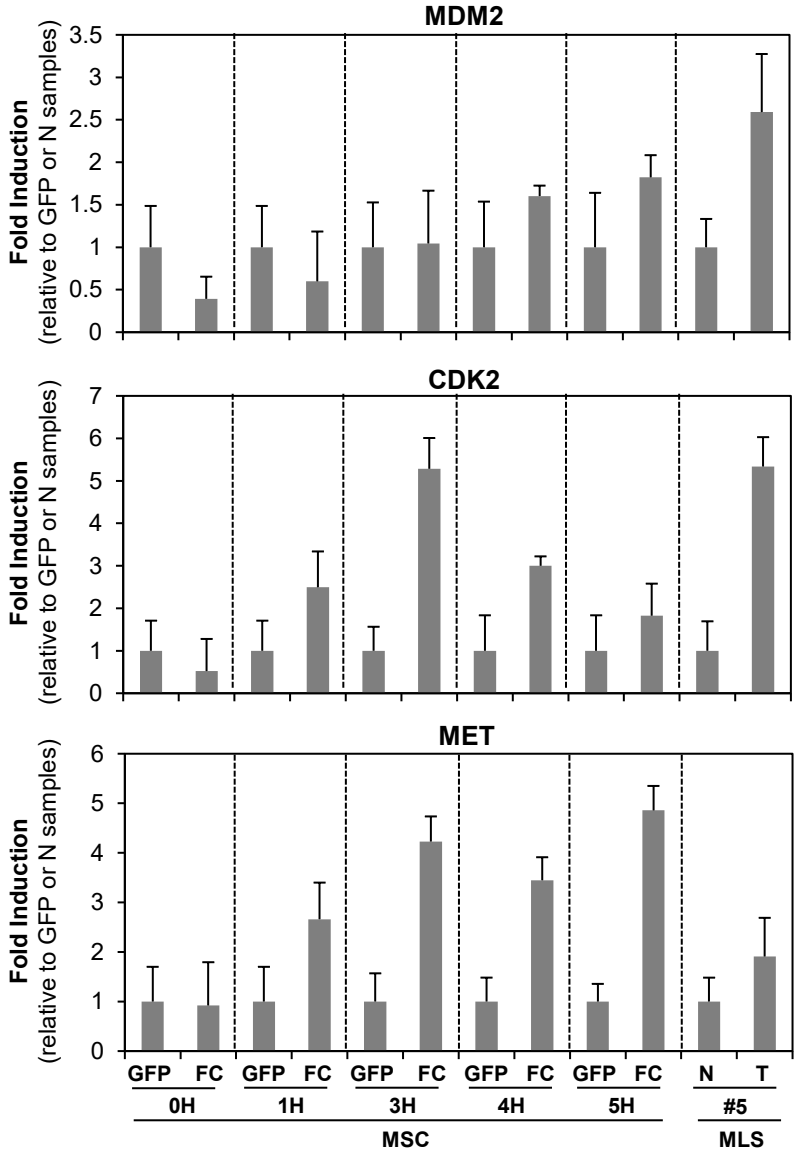

Supplementary Figure 6. Expression of MDM2, CDK2 and MET in FC-expressing hMSCs. RT-qPCR analysis showing the fold induction of MDM2, CDK2 and MET in the indicated FC-expressing hMSCs and human MLS samples (MLS#5 and #6) relative to their corresponding GFP-hMSCs or control samples (N & T: normal and tumoral samples obtained from the same patient).

Rodriguez et al. **Supplementary Figure 7**

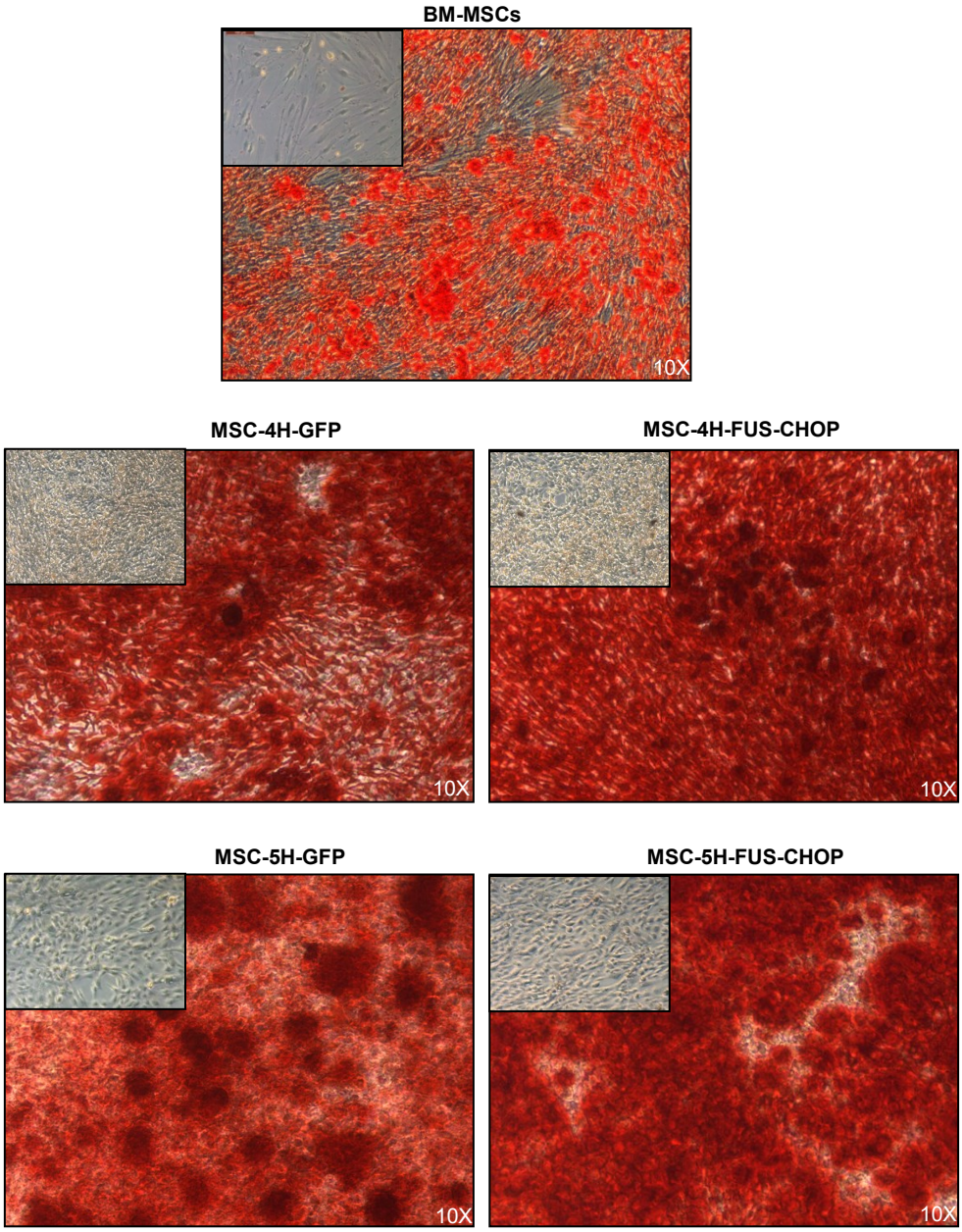

Supplementary Figure 7. Osteogenic differentiation of control and FC-expressing hMSCs. Representative images of GFP- and FC-expressing MSC-4H and MSC-5H cells following 14 days culture in osteogenic medium (or control medium in insets) and Alizarin Red S staining. These transformed MSCs displayed an osteogenic potential similar to wt BM-MSCs.

		MSC-0H-FC vs wt	MSC-5H-FC vs wt	T-5H-FC vs wt
Gene Name	Entrez Gene ID	Fold Change		
SERPINB2	5055	5.9421	7.0642	6.7838
NPTX1	4884	5.5889	11.6482	10.3386
ACTG2	72	5.0298	6.4612	7.573
DHRS9	10170	4.8463	4.5419	7.5103
TUBAL3	79861	4.7958	2.3487	4.3376
PCSK1	5122	4.621	5.2328	2.6207
DIRAS3	9077	4.559	2.0268	2.6363
WDR69	164781	4.1424	5.0399	3.8808
SERPINA9	327657	4.0606	4.7691	6.1522
IL33	3553	3.9088	6.1959	4.7588
MYH2	4620	3.8204	-2.7625	-3.017
IGFBP1	3484	3.5269	4.9014	6.0437
CHI3L2	1117	3.5226	3.6826	4.1232
SPP1	6696	3.3822	3.4302	2.5901
EREG	2069	3.3408	9.0725	9.4533
GJB2	2706	3.3354	6.2643	8.9412
MYCT1	80177	3.3305	4.3955	6.0597
ANO1	55107	3.3205	-2.1768	-2.187
ITGA2	3673	3.2333	4.6117	5.2591
HLA-DRA	3122	3.1878	5.4362	4.0499
HLA-DRB5	3127	3.1712	7.1837	6.2169
FBXL16	146330	3.1294	4.0243	5.6507
PRSS3	5646	3.1108	5.7531	5.9334
GLDN	342035	3.0001	-2.7468	-2.7082
HLA-DRB4	3126	2.9071	4.3642	3.4076
IL1RL1	3552	2.8833	6.0495	9.1528
AREG	727738	2.8553	7.1881	7.5961
FAM65C	140876	2.8383	8.6223	8.26
CXCL6	6372	2.792	9.9077	8.1462
DNER	92737	2.6736	12.0048	10.8256
KPRP	448834	2.6722	5.2283	5.5736
COL17A1	1308	2.6451	6.0832	7.1257
CCL20	6364	2.6104	4.8194	5.1284
IL1A	3576	2.6064	9.0197	10.3281
F2RL1	2150	2.5899	7.1443	7.5947
FAM159B	100132916	2.4632	4.1192	5.816
AGPAT9	84803	2.4551	5.1741	6.1592
SYT1	6857	2.4453	5.1219	4.5967
TFPI2	7980	2.3736	3.4032	3.326
SHISA2	387914	2.3699	2.1986	2.7519
IL8	9173	2.3594	12.69	12.0155
ESM1	11082	2.3511	3.3024	3.0988
CRHBP	1393	2.3482	2.4191	2.0724
IL1B	90865	2.326	11.6203	11.3889
TSPAN13	27075	2.2625	3.6106	4.5706
TMEM233	387890	2.2488	4.1663	5.8583
FAM167A	83648	2.2158	4.711	2.2683
LTF	4057	2.1967	-2.2319	-3.6469
TSLP	85480	2.1555	2.0544	3.3399
PDE10A	10846	2.1473	2.6294	3.3533
GREM1	26585	2.0987	-2.5645	-2.1933
GRB14	2888	2.0805	2.4921	2.3904
ALDH1A3	220	2.0725	3.1294	2.9035
ETV1	2115	2.0723	3.0987	4.0146
GALNT3	2591	2.0712	2.4273	2.7548
RAB38	23682	2.05	6.8926	7.9073
SEMA3A	10371	2.0457	3.5455	3.939
PAQR9	344838	2.0329	5.0011	3.5433
COLEC12	81035	2.0017	7.3735	6.903
RIMS3	9783	-2.0142	-4.6488	-4.3715
TNNT3	7140	-2.075	-2.117	-2.1825
PIEZO2	63895	-2.0826	-8.4943	-8.2146
GPM6B	2824	-2.1002	-6.4877	-6.4788
OLFML2B	25903	-2.1027	-2.8754	-3.9638
NPY2R	4887	-2.1076	-2.8814	-2.888
C11orf96	387763	-2.1145	-4.186	-3.771
LINGO1	84894	-2.1583	-7.0423	-6.9643
INMT	11185	-2.2948	-8.0877	-5.8159
BZRAP1	9256	-2.3451	-5.4808	-5.0606
LRRC4C	57689	-2.4366	-3.2549	-3.6032
PADI2	11240	-2.4788	-5.9956	-5.1952
TSHR	7253	-2.5296	-3.5563	-3.5326
RASL12	51285	-2.5877	-2.8407	-2.848
RANBP3L	202151	-2.6073	-4.5506	-4.8353
TSPAN15	23555	-2.6316	-4.4418	-3.1822
APCDD1	147495	-2.8147	-2.8146	-2.3377
ENTPD1	953	-2.817	-5.6024	-5.3646
RSPO1	284654	-2.884	-3.1153	-3.1143
MBL2	4153	-2.978	-3.5742	-3.1725
TTC21A	199223	-3.0097	-2.9672	-3.1658
TM6SF1	53346	-3.1443	-2.5898	-3.793
RFPL4B	442247	-3.529	-2.5073	-3.2263
STEAP4	79689	-3.5673	-3.5924	-3.4745
FOLR1	2348	-3.5871	-5.1069	-3.2403
FOS	2353	-3.8515	-4.0025	-3.4707
ADAD2	161931	-3.9135	-3.8443	-4.1093
ICAM5	7087	-4.2885	-2.4132	-3.12
USF1	7391	-4.565	-3.9469	-3.8941
ZNF556	80032	-4.8381	-4.8284	-4.5313
MPPED1	758	-5.2334	-5.7056	-5.745
BOLL	66037	-5.4149	-5.0559	-5.3253

Supplementary Figure 8. List of the 91 genes commonly altered in MSC-0H-FC, MSC-5H-FC and T-5H-FC cells. This group of genes represents the FC-specific contribution to the MLS model. Green/red colors indicate down-/up-regulation of these genes. The fold change values are indicated.